Journal of Contaminant Hydrology 99 (2008) 49–67

Contents lists available at ScienceDirect

Journal of Contaminant Hydrology

journal homepage: www.elsevier.com/locate/jconhyd

Distribution and variability of redox zones controlling spatial variability of arsenic in the Mississippi River Valley alluvial aquifer, southeastern Arkansas

M.U. Sharif [a,*], R.K. Davis [a,1], K.F. Steele [a,1], B. Kim [a,1], P.D. Hays [a,1], T.M. Kresse [b,2], J.A. Fazio [c,3]

[a] Environmental Dynamics Program, University of Arkansas, Fayetteville, AR 72701, USA
[b] U S Geological Survey, Arkansas Water Science Center, Little Rock, AR 72211, USA
[c] Water Division, Arkansas Department of Environmental Quality, Little Rock, AR 72219, USA

ARTICLE INFO

Article history:
Received 16 May 2007
Received in revised form 12 February 2008
Accepted 5 March 2008
Available online 20 March 2008

Keywords:
Arsenic (As)
Aquitard
Sequential extraction
Recharge potential
Redox

ABSTRACT

Twenty one of 118 irrigation water wells in the shallow (25–30 m thick) Mississippi River Valley alluvial aquifer in the Bayou Bartholomew watershed, southeastern Arkansas had arsenic (As) concentrations (<0.5 to 77 μg/L) exceeding 10 μg/L. Sediment and groundwater samples were collected and analyzed from the sites of the highest, median, and lowest concentrations of As in groundwater in the alluvial aquifers located at Jefferson County, Arkansas. A traditional five-step sequential extraction was performed to differentiate the exchangeable, carbonate, amorphous Fe and Mn oxide, organic, and hot HNO_3-leachable fraction of As and other compounds in sediments. The Chao reagent (0.25 M hydroxylamine hydrochloride in 0.25 M HCl) removes amorphous Fe and Mn oxides and oxyhydroxides (present as coatings on grains and amorphous minerals) by reductive dissolution and is a measure of reducible Fe and Mn in sediments. The hot HNO_3 extraction removes mostly crystalline metal oxides and all other labile forms of As. Significant total As (20%) is complexed with amorphous Fe and Mn oxides in sediments. Arsenic abundance is not significant in carbonates or organic matter. Significant (40–70 μg/kg) exchangeable As is only present at shallow depth (0–1 m below ground surface). Arsenic is positively correlated to Fe extracted by Chao reagent (r=0.83) and hot HNO_3 (r=0.85). Arsenic extracted by Chao reagent decreases significantly with depth as compared to As extracted by hot HNO_3. Fe (II)/Fe (the ratio of Fe concentration in the extracts of Chao reagent and hot HNO_3) is positively correlated (r=0.76) to As extracted from Chao reagent. Although Fe (II)/Fe increases with depth, the relative abundance of reducible Fe decreases noticeably with depth. The amount of reducible Fe, as well as As complexed to amorphous Fe and Mn oxides and oxyhydroxides decreases with depth. Possible explanations for the decrease in reducible Fe and its complexed As with depth include historic flushing of As and Fe from hydrous ferric oxides (HFO) by microbially-mediated reductive dissolution and aging of HFO to crystalline phases. Hydrogeochemical data suggests that the groundwater in the area falls in the mildly reducing (suboxic) to relatively highly reducing (anoxic) zone, and points to reductive dissolution of HFO as the dominant As release mechanism. Spatial variability of gypsum solubility and simultaneous SO_4^{2-} reduction with co-precipitation of As and sulfide is an important limiting process controlling the concentration of As in groundwater in the area.

1. Introduction

Following the accumulation of evidence for the chronic toxicological health effects of arsenic (As) in drinking water, including cancer, the US Environmental Protection Agency (U.S. EPA) reduced the MCL for As from 50 to 10 μg/L (U.S. EPA, 2001). Most municipal-supply water systems in eastern Arkansas draw water from deeper Tertiary aquifers (91–213 m below ground

* Corresponding author. Current address: GENIVAR, 600 Cochrane Drive, Suite 500, Markham, Ontario, Canada L3R 5K3. Tel.: +1 416 436 3942.
E-mail address: md.sharif@gmail.com (M.U. Sharif).
[1] Current address: Department of Geosciences, University of Arkansas, Fayetteville, AR 72701, USA.
[2] Current address: USGS, Water Science Center, 401 Hardin Road, Little Rock, AR 72211, USA.
[3] Current address: Arkansas Dept. of Envi. Quality, 8001 National Drive, Little Rock, AR 72219, USA.

0169-7722/$ – see front matter © 2008 Elsevier B.V. All rights reserved.
doi:10.1016/j.jconhyd.2008.03.001

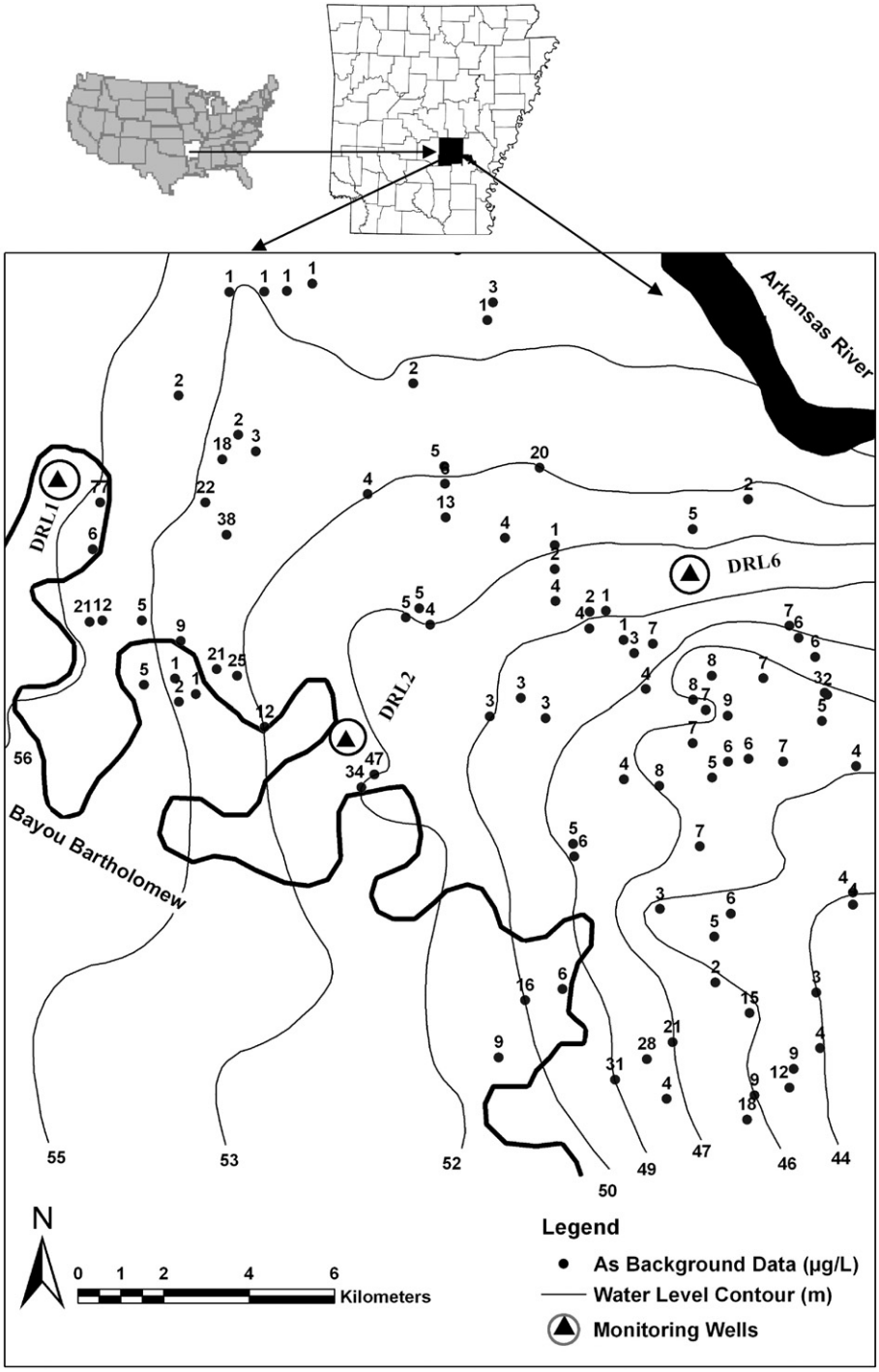

Fig. 1. Location of study area, monitoring wells sites, water level map, and As background data. Location map (Jefferson County, AR, USA) of the study area, which shows As background data in µg/L (solid circle), water level contour in meter (thin solid line), monitoring wells (solid triangle in open circle), river and water courses (thick dark black lines).

surface) where As is generally <0.5 µg/L. Impacts from As to municipal-supply water systems in Arkansas are low. However, the potential health impact of As to drinking water supply systems in Arkansas is still significant. Approximately 200 public water supply wells screened in the shallow Mississippi River Valley alluvial aquifer (herein referred to as the alluvial aquifer) serve about 450,000 people. These public water supply wells include commercial hunting camps, gasoline stations, trailer parks, and restaurants, as well as most private domestic wells. Recent publications documenting water quality in the Bayou Bartholomew watershed of southeastern Arkansas (Kresse and Fazio, 2002) revealed that 21 out of 118 irrigation water wells

installed in the shallow alluvial aquifer (25–30 m) had As concentrations >10 μg/L. Kresse and Fazio (2003) provide evidence for reductive dissolution of hydrous ferric oxides (HFO), and release of sorbed and/or co-precipitated trace metals as the source of soluble As in the alluvial aquifer. Their evidence is mainly based on observed statistical correlations between As and various redox-sensitive parameters (NO_3^-–N, NH_4–N, and Fe) favorable for reductive dissolution of HFO. These results are similar to alluvial environments in other parts of USA and abroad. The data of Kresse and Fazio (2002) indicate that domestic wells completed in alluvial aquifer may present risks to at least 18% of the private well owners not protected by the Safe Drinking Water Act (SDWA), and increased treatment costs for those public water supplies installed in this alluvial aquifer.

This work expands that of Kresse and Fazio (2003) by focusing on the hypothesis of As mobilization caused by reductive dissolution of HFO (Matisoff et al., 1982; Korte, 1991) and transport of As in a specific area of the alluvial aquifer within the Bayou Bartholomew watershed with the highest known concentrations of As. This study is unique in that it is the first detailed study of the transport and fate of As in a large alluvial aquifer that has relatively low to moderate As concentrations (<0.5–50 μg/L) in comparison with other better known alluvial aquifers with As pollution, such as Bangladesh (2.5–846 μg/L; Ahmed et al., 2004).

2. Study area

The study area is about 225 km^2 in the southern part of Jefferson County, Arkansas (Fig. 1). It is bounded by the Arkansas River to the northeast and Bayou Bartholomew to the southwest. The area comprises the northeastern part of the Bayou Bartholomew watershed, which is covered almost entirely by Holocene alluvial deposits of the Mississippi and Arkansas Rivers. The Holocene alluvial deposits are represented by downward coarsening from clays, silts and fine sand at the surface (herein referred to as surface aquitard), to coarse sand and gravel at the base. Pleistocene alluvial deposits of the Mississippi and Arkansas Rivers form terraces with minor exposures of Tertiary-age strata along topographically high areas, and are found beyond the western part of the study area (Kresse and Fazio, 2002). The thickness of the surface aquitard varies from <6 to 12 m (Fig. 2), and permeability of the aquitard is heterogeneous due to varying proportions of clay, silt, and fine sands. Where the surface aquitard is thick and less permeable, it forms a confining unit which impedes recharge to the alluvial aquifer. The thickness of the alluvial aquifer ranges from 18 to 43 m (Kleiss et al., 2000). Channel fill, point bar, and back swamp deposits associated with present and former channels of the Mississippi and Arkansas Rivers produced abrupt changes in lithology and resulted in large

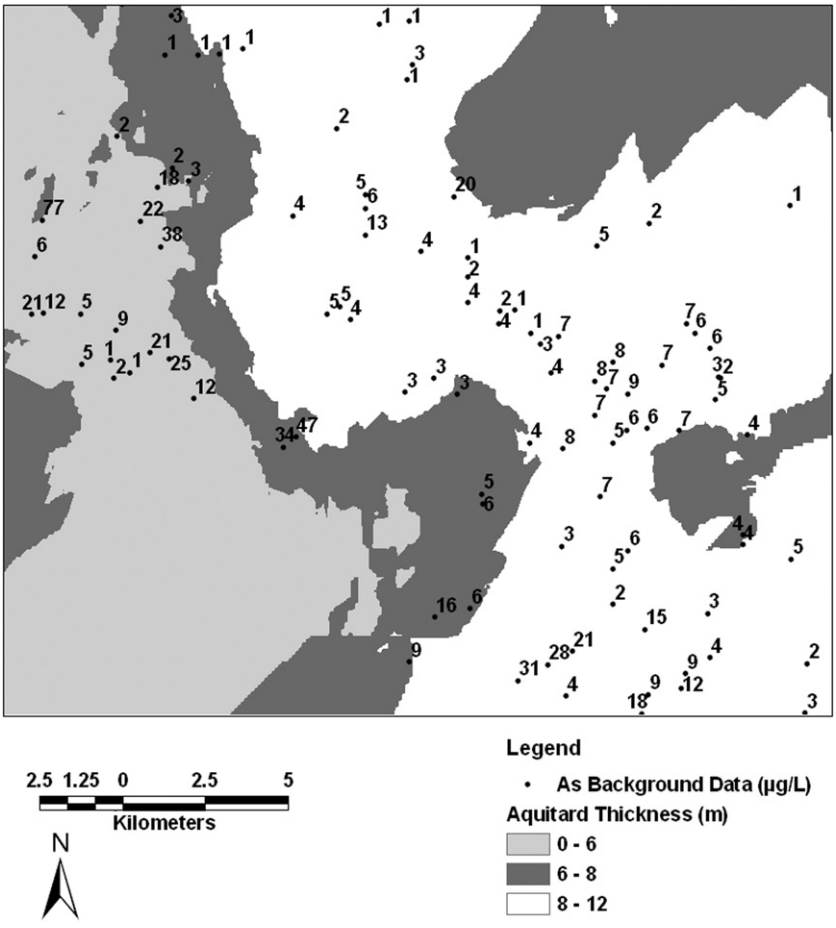

Fig. 2. Aquitard thickness and As background data in the study area. Map shows As background data in μg/L (solid circle) and surface aquitard thickness in meter (the black color as 6–8 m, the gray color as 0–6 m, and the white color as 8–12 m).

spatial and vertical variations in the hydraulic properties of the aquifer system (Joseph, 1999). The regional direction of groundwater flow is generally to the south and east except where affected by intense groundwater withdrawals (Schrader, 2001). Local perturbations in flow directions result from the influent–effluent character of smaller streams within the study area. Row-crop agriculture represents the major land use in the floodplain, whereas silviculture dominates the land use in the terrace portion of the watershed. Eastern Arkansas receives an annual precipitation of 1.2 to 1.4 m (Freiwald, 1985). Reliance on water from the alluvial aquifer for crop production has increased dramatically over recent years. The increase in estimated groundwater withdrawals from 1985 to 1995 was about 45% (Schrader, 2001).

3. Materials and methods

3.1. Site selection

Within the 225 km^2 study area three contrasting sites for nested monitoring wells (two wells at 10 m and 36 m deep below ground surface, respectively) were selected as a high As (>50 μg/L) area in the northwest (DRL1), a medium As (10–50 μg/L) area in the south (DRL2), and a low As (<10 μg/L) area in the northeast (DRL6). These locations for monitoring wells were selected based on As background data (Kresse and Fazio, 2002) of 118 water wells, geologic cross sections prepared from borehole logs of Arkansas Geologic Commission (AGC), groundwater flow maps, distribution of surface aquitard, and primary recharge areas. Three pairs of nested monitoring wells were drilled, installed, developed, and sampled at the selected sites in February 2006. The capital letter "D" and "S" are used after the site designation letters (DRL1, DRL2 or DRL6) to describe deep and shallow monitoring wells (e.g. DRL1S, DRL1D, etc.), respectively.

3.2. Collection of cores

A hollow stem auger drill rig equipped with a 152 cm long and 7.62 cm outside diameter (O.D.) CME® sampler (steel) was used to extract continuous sediment cores to a depth of 12 m. The same rig equipped with a 46 cm, split-spoon sampler accepting a 5 cm O.D. steel liner was used to collect cores at approximately150 cm intervals to a depth of 36.5 m. No drilling fluid was used to minimize borehole contamination. Core recovery using the CME® sampler was 80% or greater, while a varying rate of 30% to 90% core recovery was achieved with the split-spoon sampler. The lower-volume core recovery was due to the increase of fine sand fractions which flowed from the core barrel even with the use of sediment traps (egg shells or one-way valves). The extracted cores were collected, wrapped in aluminum foil, labeled, and transported to the laboratory for physical and chemical analysis. A sub-sample (about 200 g) of each core was also separated in the field into plastic Ziploc® bags, and preserved below 4 °C to provide fresh sample for Fe speciation, and comparison between extraction procedures using dry and fresh wet sediments. Sediment samples were labeled numerically after the monitoring well ID (e.g. DRL1S1, DRL1S2).

3.3. Monitoring wells

At each site two monitoring wells with 5 cm O.D. PVC pipe were installed at a depth of 10.6 m and 36.5 m below ground surface, respectively. The shallow wells were screened from 4.6 to 10.6 m, and the deep wells were screened from 33.5 to 36.5 m. Each aspect of monitoring well installation was completed by standard procedures (Wayne et. al., 1997) and complied with federal, state, and local regulations. The depth to groundwater was measured with a Solinst® Model 101 meter. Accurate groundwater elevation was calculated from post-processed land-surface elevation data. The land-surface data, with an estimated precision of ±2 cm, were generated by survey-grade Trimble® 4000SSE GPS units using the Fast Static method of data collection. The same GPS units were used to acquire land-surface elevation data used in the preparation of a detailed groundwater flow map, which was based on measurement of depth to groundwater at 174 water

Table 1
Groundwater parameters measured in the field

Parameters	Units	Instrument and model	Methods
Temperature	°C	YSI® Model 30 handheld Salinity, Conductance, and Temperature Meter	
EC	μS/cm		
pH		Multi Probe Orion® 3-Star portable pH/ORP meter	
ORP	RmV		
DO	mg/L	YSI® 550A Dissolved Oxygen meter	
Alkalinity	mg/L as $CaCO_3$	HACH® Digital Titrator	HACH Method 8203
Dissolved S^{2-}	μg/L		HACH 8131 (Methylene Blue)
Fe^{2+}	mg/L		HACH 8146 (1, 10 Phenanthroline)
Fe (total)	mg/L		HACH 8008 (FerroVer)
Mn^{2+}	mg/L	HACH® spectrophotometer (DR 2800)	HACH 8148 (Periodate Oxidation)
Inorganic As speciation	μg/L	Separated using Anion exchange columns and measured by ICP-MS	Edwards et al. (1998)
Inorganic and organic As speciation	μg/L	Separated using Anion and Cation exchange columns and measured by ICP-MS	Grabinski (1981)
Volatile organic and inorganic C	ppm	Thermo® TVA-100B Toxic Vapor Analyzer, which uses both Flame Ionization Detector (FID) and Photo Ionization Detector (PID)	

wells in the study area. The monitoring wells were initially developed using a PVC bailer attached to the wire-line on the drill rig, and secondarily using a Redi-Flo® VFD GRUNDFOS pump.

3.4. Groundwater sampling, field monitoring, and laboratory analyses

All chemical analyses were performed on groundwater samples collected from the monitoring wells with a generator-driven submersible pump (Redi-Flo® VFD GRUNDFOS) in June 2006. Sample collection, handling, and preservation procedures of United States Geological Survey (Shelton and Chapel, 1994) were followed to ensure data quality and consistency. Prior to sample collection, the well was pumped continuously for 30–45 min until the temperature, electrical conductance (EC), pH, oxidation–reduction potential (ORP), and dissolved oxygen (DO) readings stabilized within the accepted guidelines of NAWQA. After recording readings of these stabilized monitoring parameters, a number of other redox-sensitive chemical parameters including Fe and As speciation, Mn^{2+}, dissolved S^{2-}, volatile organic carbon (Table 1) were measured in the field.

3.5. Collection of groundwater samples for total analysis

A set of four groundwater samples were collected in 100 ml HDPE bottles, that were (1) filtered (0.45 μm) and acidified (2) not-filtered and acidified (3) filtered (0.20 μm) and acidified, and (4) filtered (0.45 μm) and not-acidified. Acidification was achieved by adding concentrated HNO_3 (VWR® Omni trace grade) until pH reached 2 or less standard units. Dissolved cations including Ca^{2+}, Mg^{2+}, Na^{+}, K^{+}, SiO_2, Mn^{2+}, Fe^{2+}, Al^{3+}, Ag, B, Ba, Be, Cd, Cr, Cu, Li, Ni, Mo, Pb, Se, Sb, Sr, Ti, Zn, V, and As were measured on the acidified samples by Inductively Coupled Plasma Mass Spectrometer (ICP-MS) following EPA method 200.8. Dissolved anions including Cl^{-}, Br^{-}, F^{-}, SO_4^{2-}, NH_4–N, NO_3^{-}–N, PO_4^{3-}–P were measured on the non-acidified samples by Ion Chromatograph following standard EPA method Anion 300.0. TOC was measured by a TOC analyzer using the liquid sample module. Filtering was done using two disposable syringes with filters (0.45 μm and 0.20 μm). Both filtered and non-filtered samples were analyzed by ICP-MS to identify the difference between the total and dissolved fraction of metals (e.g. As, Fe) in groundwater. Two filter sizes (0.45 μm and 0.20 μm) were used to

Table 2
Chemical data for groundwater in the monitoring wells

Parameter	DRL1S	DRL1D	DRL2S	DRL2D	DRL6S	DRL6D
Water level (m bls)	5.6	5.7	6.9	6.8	8.4	8.3
Temperature (°C)	18.5	17.9	19.5	18.5	18.9	18.5
EC (μS/cm)	310	306	456	426	953	658
TDS (mg/L)	209	187	261	241	572	382
pH	6.11	6.13	6.87	6.81	6.84	6.68
Alkalinity (mg/L as $CaCO_3$)	108	135	215	189	437	300
ORP (RmV)	198	124	55	66	−247	−223
DO (mg/L)	0.4	0.08	0.06	0.06	0.08	0.08
Hardness (mg/L)	102	61	177	164	426	278
Total dissolved As (μg/L)	0.73	29.6	12.3	39.7	49.4	1.02
As(III) (μg/L)	<0.5	10.2	1.14	8.22	5.23	<0.5
As(V) (μg/L)	0.7	20.3	11.4	33.9	45.3	1.15
Particulate As (μg/L)	0.1	0	0	2.2	0	0.3
Total Fe (mg/L)	1.9	41	11.5	16.3	8.3	11
Fe^{2+} (mg/L)	0.04	9.2	7.3	8.5	4.6	5.8
Fe^{3+} (mg/L)	1.6	31.8	4.2	7.8	2.8	3.9
Particulate Fe (mg/L)	0.24	1.7	0.1	0	0.16	0.3
Ca^{2+} (mg/L)	25.4	17.4	55.6	48.8	130	80
Mg^{2+} (mg/L)	9.3	4.4	9.4	10.3	24.7	18.9
Na^{+} (mg/L)	16.3	11.7	16.3	17.1	41.8	18.7
K^{+} (mg/L)	2	2.6	1.1	1.4	1.5	1.2
Mn^{2+} (mg/L)	2.7	1.5	0.5	0.7	0.4	0.7
Cl^{-} (mg/L)	14.2	20.1	7.7	7.6	27.1	29.6
SO_4^{2-} (mg/L)	18	2	1	1.4	46	1.4
NO_3^{-}–N (mg/L)	2.25	<0.01	<0.01	<0.01	<0.01	<0.01
NH_3–N (mg/L)	0.03	0.21	0.9	0.35	1.1	0.72
PO_4–P (mg/L)	0.02	0.03	0.03	0.05	0.02	0.05
S^{2-} (μg/L)	2	6	11	51	27	27
SiO_2 (mg/L)	31.7	32.9	31.6	34	34.4	28.3
Br^{-} (mg/L)	0.08	0.08	0.06	0.06	0.14	0.12
Ba^{2+} (μg/L)	166	198	215	150	538	388
B^{3+} (μg/L)	25	13	35	30	42	44
Fl^{-} (mg/L)	0.4	0.3	0.3	0.4	<0.01	0.3
Zn^{2+} (μg/L)	2.7	5.2	2.4	3.8	1.7	1.4
V^{5+} (μg/L)	0.96	0.51	<0.50	<0.50	<0.50	<0.50
Co^{2+} (μg/L)	1.95	6.44	0.52	<0.50	<0.50	<0.50
Ni^{2+} (μg/L)	2.7	4.4	<0.50	<0.50	<0.50	<0.50
TOC (mg/L)	6.2	6.8	6	6.3	11	6.8
VOC (mg/L)	<0.1	<0.1	0.3	0.5	1.4	0.7

identify the difference in stripping of metallic ions from the suspended particles in groundwater. All groundwater samples were analyzed in the Arkansas Department of Environmental Quality (ADEQ) laboratory, Little Rock, AR. Standard calibrations were based on standard addition for all dissolved ions analyzed in the laboratory. Chemical data of groundwater samples are given in Table 2.

3.6. Preparation of sediment samples and laboratory analysis

Sealed sections (wrapped in aluminum foil) of the stored core samples were opened and sub-sampled in February 2006 for grain size, porosity, and geochemical analyses. About 100 g of stored sediment from each core were separated and dried below 40 °C in an oven. The sediments were crushed by a

Table 3
As concentration (mg/kg) from Tessier's sequential extraction and a separate single extraction of hot HNO_3 and H_2SO_4

Depth (m)	Lithology	Exchangeable	Carbonates	Amorphous Fe+Mn oxide oxides	Organic	Hot HNO_3 leachable	Extraction total	Hot HNO_3 and H_2SO_4
DRL1								
0	Sandy silt	<0.037	0.31	0.47	0.22	0.75	1.44	1.59
0.3	Silty sand	0.05	<0.37	5.98	5.25	4.45	16.7	18.1
0.6	Silty sand	<0.037	<0.37	0.45	0.16	1.11	1.73	2.10
2.1	Clayey silt	<0.037	<0.37	0.38	0.13	2.09	2.60	2.95
3	Clayey silt	<0.037	<0.37	0.41	0.15	1.83	2.39	3.01
4.9	Sandy silt	<0.037	<0.37	0.53	<0.12	1.07	1.60	3.18
6.1	Clayey silt	<0.037	<0.37	0.68	<0.12	1.74	2.42	2.38
7	Clayey silt	<0.037	<0.37	0.57	<0.12	2.88	3.44	2.63
7.6	Silty sand	<0.037	<0.37	0.25	<0.12	0.79	1.04	4.10
8.8	Sand	<0.037	<0.37	0.52	<0.12	1.62	2.18	1.97
10.1	Sand	<0.037	<0.37	0.24	<0.12	0.78	1.02	2.09
13.7	Sand	<0.037	<0.37	<0.12	<0.12	0.23	0.23	<0.5
16.8	Sand	<0.037	<0.37	0.13	<0.12	0.25	0.37	<0.5
18.3	Sand	<0.037	<0.37	0.46	<0.12	1.04	1.50	<0.5
21.3	Clay lens	<0.037	<0.37	0.50	<0.12	4.55	5.05	0.79
24.4	Sand	<0.037	<0.37	<0.12	<0.12	0.14	0.14	4.33
25.9	Sand	<0.037	<0.37	0.21	<0.12	0.31	0.51	<0.5
33.5	Sand	<0.037	<0.37	0.14	<0.12	0.36	0.50	<0.5
36.4	Sand	<0.037	<0.37	0.17	<0.12	1.15	1.32	<0.5
36.6	Clay lens	<0.037	<0.37	1.10	<0.12	3.38	4.55	1.35
DRL2								
0.0	Silt	0.07	<0.37	0.99	<0.12	1.99	3.05	3.35
0.8	Sandy silt	<0.037	<0.37	0.44	<0.12	1.91	2.59	2.58
1.5	Clayey silt	<0.037	<0.37	0.49	<0.12	2.10	3.99	3.68
2.4	Sandy silt	<0.037	<0.37	0.99	<0.12	3.40	2.35	3.15
4.0	Clayey silt	<0.037	<0.37	1.14	<0.12	2.85	4.39	3.78
5.5	Sandy silt	0.06	<0.37	0.46	<0.12	1.59	2.11	2.58
6.4	Clayey silt	<0.037	<0.37	0.61	<0.12	2.58	3.19	1.67
7.6	Silt	<0.037	<0.37	0.56	<0.12	1.72	2.28	1.53
9.1	Sand	<0.037	<0.37	<0.12	<0.12	0.27	0.27	<0.5
10.7	Sand	<0.037	<0.37	0.65	<0.12	3.60	4.25	1.80
12.2	Sand	<0.037	<0.37	<0.12	<0.12	0.27	0.27	<0.5
13.7	Clayey silt	<0.037	<0.37	<0.12	<0.12	0.13	0.13	<0.5
15.2	Sand	<0.037	<0.37	<0.12	<0.12	0.13	0.13	<0.5
18.3	Clay	<0.037	<0.37	0.59	<0.12	1.37	1.96	0.79
21.3	Sand	0.05	<0.37	0.37	<0.12	1.00	1.42	0.70
30.5	Sand	<0.037	<0.37	0.12	<0.12	0.20	0.20	<0.5
DRL6								
0.0	Sandy silt	0.07	<0.37	0.28	<0.12	1.92	2.27	2.42
0.6	Silt	<0.037	<0.37	0.28	<0.12	1.79	2.07	2.10
1.1	Clayey silt	0.08	<0.37	1.45	<0.12	5.45	6.98	4.43
5.5	Sandy silt	<0.037	<0.37	0.27	<0.12	0.47	0.74	<0.5
7.3	Clayey silt	<0.037	<0.37	2.22	<0.12	3.53	5.75	2.38
8.2	Silty clay	0.04	<0.37	0.84	<0.12	1.92	2.80	1.14
10.4	Clayey sand	<0.037	<0.37	0.43	<0.12	0.70	1.12	0.56
10.7	Clayey sand	<0.037	<0.37	0.33	<0.12	0.86	1.19	0.56
11.0	Silty sand	<0.037	<0.37	0.21	<0.12	0.46	0.67	<0.5
12.2	Silty sand	0.04	<0.37	5.10	<0.12	22.8	27.9	9.30
12.8	Sand	<0.037	<0.37	2.02	<0.12	2.40	4.42	2.63
15.2	Sand	<0.037	<0.37	0.25	<0.12	0.61	0.86	0.68
24.4	Sand	<0.037	<0.37	0.64	<0.12	1.83	2.46	1.51
27.4	Sand	<0.037	<0.37	0.17	<0.12	0.45	0.62	<0.5
30.5	Sand	0.06	<0.37	0.26	<0.12	0.90	1.22	0.94
36.6	Sand	0.06	<0.37	0.24	<0.12	0.79	1.09	0.91

conventional porcelain pestle and mortar, and passed through a 1 mm nylon screen. These screened sediment samples were used for a sequential extraction procedure for major cations and trace metals, including As. Grain size analysis was done with little or no crushing on dried pre-screened samples by using a micro pipette method (Miller and Miller, 1987). Porosity was measured by weighing 50 ml hand-packed sediments in a graduated cylinder. Water was slowly added to the 50 ml mark and the sample was shaken to remove air bubbles and saturate evenly with water. Gravimetric porosity [$(1-(\rho_b/\rho_s)]$] was calculated by mean particle density (ρ_s = mass of solids/volume of solids) and dry bulk density (ρ_b = mass of dry solids/volume of dry solids). The five-step sequential extraction (modified from Tessier et al., 1979; Chao and Zhou, 1983; Miller, 2001) was conducted using 2 g dry sediment. The steps of the extraction procedures are designed to specific environmental compartments of As and other trace metals in the sediments, which are as follows:

1. Exchangeable: 16 ml of 1 M sodium acetate to pH 8.2 for 1 h.
2. Associated with carbonates: 16 ml of 1 M sodium acetate to pH 5 for 4 h.
3. Attached to amorphous Fe and Mn oxides: 40 ml of 0.25 M NH_2–OH–HCl (hydroxylamine hydrochloride) in 0.25 M HCl; heat to 50 °C for 30 min. The reagents used here are referred to as "Chao reagent" described in the extraction procedures of Chao and Zhou (1983).
4. Bound to organic matter: 6 ml of 0.02 M HNO_3 and 10 ml of 30% H_2O_2 to pH 2 with HNO_3; heat to 85 °C for 2 h, and later 6 ml of 30% H_2O_2; heat to 85 °C for 3 h.
5. Hot HNO_3 leachable: 15 ml of 7 M HNO_3 for 2.5 h at 70 °C for the first 30 min and later at 100 °C for the next 2 h.

The last step of the sequential extraction (hot HNO_3 extraction) was used to represent the least environmentally-available As. A total of 60 sediment samples were extracted. Five duplicates, one gravel-pack sample, a bentonite grout sample, eight wet sediment samples preserved in the freezer, and two coarse (>1 mm) sediment samples were also extracted for quality control and comparison purposes. The extracted solutions were shipped to the ADEQ laboratory in Little Rock, Arkansas for analysis by ICP-MS. Sediment extraction data are listed in Table 3.

3.7. XRD and SEM analysis

Dried sediment samples were powdered using a grinding mill (RockLabs®) for X-ray Diffractometry (XRD) and Scanning

Table 4
Total organic carbon and reduced inorganic sulfur analyses results

Lithology	Depth (m)	*TC (%)	*TIC (%)	*TOC (%)	*IS (%)	Remarks
DRL6						
Sandy silt	0	ND	ND	ND	*ND	No sediment sulfide is detected above the water table. Sediment sulfide is present below the water table. Significant sediment sulfide is also present in sands at depths.
Clayey silt	1.1	1.20	1.04	0.16	*ND	
Sandy silt	5.8	0.18	<0.1	<0.1	*ND	
Clayey sand	7.3	0.97	0.16	0.81	0.043	
Silty clay	8.2	0.84	0.12	0.72	<0.01	
Clayey sand	10.1	0.18	ND	0.18	*ND	
Silty sand	11	<0.1	ND	<0.1	*ND	
Sand	12.8	<0.1	ND	<0.1	0.032	
Clay lens	24.4	0.17	ND	0.17	<0.01	
Sand	36.6	<0.1	ND	<0.1	<0.01	
DRL2						
Silt	0.1	0.43	ND	0.43	ND	
Clayey silt	1.5	0.11	<0.1	0.11	ND	
Clayey silt	6.4	0.16	ND	0.16	ND	
Silty sand	6.7	<0.1	ND	<0.1	ND	
Silt	7.6	0.24	ND	0.24	ND	
Sand	10.7	0.67	ND	0.67	0.047	
Sand	12.2	<0.1	ND	<0.1	ND	
Sand	21	0.28	ND	0.28	<0.01	
Sand	21.3	<0.1	ND	<0.1	<0.01	
DRL1						
Sandy silt	0.1	0.17	ND	0.17	ND	
Clayey silt	2.1	0.17	ND	0.17	ND	
Clayey silt	3	0.20	ND	0.20	ND	
Sandy silt	4.9	<0.1	ND	<0.1	ND	
Clayey silt	6.1	0.10	ND	0.10	ND	
Sandy silt	6.4	<0.1	ND	<0.1	ND	
Sand	10.2	<0.1	ND	<0.1	ND	
Sand	18.3	<0.1	ND	<0.1	<0.01	
Clay lens	18.6	<0.1	ND	<0.1	0.016	
Sand	33.5	ND	ND	ND	ND	
Clay lens	36.6	0.76	ND	0.76	0.11	

*ND: Not detected.
*TC: Total carbon, TOC Analyzer, detection limit: 0.1%.
*IC: Inorganic carbon, TOC Analyzer, detection limit: 0.1%.
*IS: Inorganic sulfide, Canfield method, detection limit: 0.01%.

Table 5
Chemical parameters of groundwater generated from 23 irrigation water wells in the research area (Kresse and Fazio, 2002)

Location	Date	Al	As	Ba	B	Cr	Cu	V	Zn	Fe	Ca	Mg	Mn	K	Na	SiO_2	HCO_3
		µg/L	µg/L	µg/L	µg/L	µg/L	µg/L	µg/L	µg/L	mg/L	mg/L	mg/L	mg/L	mg/L	mg/L	mg/L	mg/L
JEF01	5/8/99	0.31	0.005	0.59	0.042	0.003	0.0009	0.0020	0.0012	10.7	143.1	32.4	0.97	2.9	71.9	32.2	514
JEF02	5/8/99	0.28	0.004	0.52	0.042	0.003	0.0007	0.0017	0.0010	7.6	102.1	25.7	0.86	2.1	54.7	32.4	439
JEF03	5/8/99	0.22	0.003	0.33	0.049	0.002	0.0005	0.0015	0.0017	5.5	74.2	20.8	0.37	1.3	31.2	35.3	386
JEF04	7/18/99	0.13	0.003	0.27	0.005	0.000	0.0046	0.0010	0.0010	15.4	48.7	10.1	0.29	1.4	26.1	36.8	224
JEF05	7/18/99	0.13	0.017	0.27	0.005	0.000	0.0005	0.0010	0.0010	23.0	48.5	10.3	0.57	1.5	22.6	35.1	222
JEF09	7/18/99	0.13	0.008	0.78	0.009	0.001	0.0014	0.0010	0.0010	10.5	134.2	33.5	0.84	1.7	64.3	29.4	442
JEF10	7/18/99	0.13	0.002	0.19	0.030	0.000	0.0005	0.0010	0.0016	3.4	48.3	12.4	0.29	0.5	17.9	36.6	240
JEF11	7/18/99	0.13	0.002	0.34	0.024	0.001	0.0011	0.0010	0.0011	5.7	90.6	22.3	1.07	0.5	33.1	28.0	415
JEF12	7/18/99	0.15	0.023	0.37	0.017	0.001	0.0005	0.0011	0.0010	10.5	113.3	20.7	0.66	0.5	12.2	24.7	451
JEF13	7/18/99	0.16	0.003	0.46	0.017	0.000	0.0005	0.0013	0.0020	12.7	100.7	24.6	1.80	0.5	26.6	32.1	464
JEF18	8/8/99	0.13	0.003	0.17	0.005	0.001	0.0005	0.0010	0.0011	15.9	23.6	7.0	0.64	1.9	29.6	32.2	129
JEF19	8/8/99	0.13	0.002	0.21	0.005	0.001	0.0005	0.0010	0.0028	12.4	22.9	5.6	0.35	2.0	23.0	36.7	117
JEF20	8/8/99	0.13	0.003	0.16	0.005	0.001	0.0005	0.0014	0.0027	8.8	21.7	8.2	0.49	2.1	18.5	30.4	128
JEF21	8/8/99	0.13	0.020	0.18	0.005	0.000	0.0005	0.0011	0.0020	8.8	27.7	7.9	1.32	2.0	16.5	51.7	150
JEF22	8/8/99	0.13	0.002	0.16	0.005	0.001	0.0005	0.0010	0.0010	29.0	10.6	4.1	0.53	2.6	10.7	29.6	63
JEF23	8/8/99	0.13	0.002	0.12	0.005	0.001	0.0006	0.0010	0.0032	8.6	38.0	6.9	0.39	2.8	15.6	32.0	172

Table 5 *(continued)*

Location	Br	Cl	F	SO_4	NH_4–N	NO_3–N	Ortho–P	Total–P	TOC	pH	Temp	EC	TDS	Hardness	Alkalinity
	mg/L	mg/L	mg/L	mg/L	mg/L	mg/L	mg/L	mg/L	mg/L		°C	µS/cm	mg/L	mg/L	mg/L as $CaCO_3$
JEF01	0.52	116.0	0.33	53.1	0.45	0.01	0.01	0.85	1.91	6.8	17.7	1353	703	491	421
JEF02	0.27	73.2	0.27	28.5	0.38	0.01	0.01	0.67	2.20	6.8	18.0	1000	522	361	360
JEF03	0.10	23.4	0.38	1.4	0.44	0.01	0.01	0.70	2.00	7.0	17.6	670	379	271	316
JEF04	0.14	23.6	0.18	10.3	0.31	0.02	0.03	0.84	1.53	6.7	17.8	451	271	163	184
JEF05	0.13	19.2	0.18	2.8	0.35	0.02	0.06	0.82	1.97	6.7	17.7	421	262	164	182
JEF09	0.42	109.4	0.27	85.2	0.33	0.02	0.01	0.64	1.82	6.8	17.9	1300	746	473	362
JEF10	0.01	11.4	0.25	2.6	0.16	0.02	0.01	0.43	1.82	6.9	18.1	413	247	172	197
JEF11	0.14	34.1	0.37	9.0	0.24	0.02	0.01	0.43	1.90	6.9	17.9	777	406	318	340
JEF12	0.07	12.8	0.23	4.0	0.40	0.02	0.01	0.50	1.84	7.1	18.0	758	402	368	370
JEF13	0.09	12.1	0.28	18.1	0.32	0.08	0.05	0.50	4.68	6.9	17.3	800	443	353	380
JEF18	0.12	22.3	0.20	14.3	0.11	0.20	0.09	0.56	1.23	6.6	17.6	317	220	88	106
JEF19	0.14	18.0	0.20	13.8	0.08	0.21	0.09	0.43	0.53	6.4	17.3	277	211	80	96
JEF20	0.01	10.6	0.20	7.6	0.05	0.87	0.06	0.31	0.33	6.5	17.7	257	199	88	105
JEF21	0.01	8.7	0.21	7.3	0.21	0.20	0.06	0.35	3.01	6.6	17.6	279	227	102	123
JEF22	0.01	9.6	0.08	7.3	0.11	0.02	0.10	0.29	1.20	6.3	17.3	148	168	43	52
JEF23	0.01	6.6	0.23	6.3	0.06	0.03	0.02	0.78	0.58	6.8	17.9	311	215	123	141

Electron Microscopy (SEM) analysis. XRD measurements used Cu Kα radiation and a graphite monochrometer on a Philips® vertical diffractometer, stepped at 0.5 s/0.02°, from 2 to 100° 2θ. Iterative identification of minerals in the samples used PC-APD® Diffraction software of Philips Analytical with search/match of the reference mineral database and generated powder patterns. Five sediment samples were magnetically separated by a Frantz® Isodynamic Separator Model L-1, and were analyzed by XRD. A subset of the magnetically separated minerals was analyzed by a Hitachi® S-2300 SEM to identify the nature of crystallinity of magnetic minerals.

3.8. Organic carbon and inorganic sediment sulfur analysis

Thirty sediment samples from three monitoring well sites were analyzed for total organic carbon (TOC) and inorganic sediment sulfur. TOC was analyzed using a Shimadzu® TOC 5050 analyzer equipped with the solid sample module (SSM 5000A). Reduced inorganic sulfur compounds (pyrite + elemental sulfur + acid volatile monosulfides) were measured by chromium reduction method or Canfield method (Canfield et al., 1986). Chromium reduction does not reduce or liberate either organic sulfur or sulfate sulfur, which makes the method specific only to reduced inorganic sulfur phases. The detection limits for TOC and inorganic sediment sulfur were 0.1% and 0.01% of sediment, respectively. Table 4 shows the results of TOC and reduced sediment sulfur in the sediments collected from the three coring sites.

3.9. Groundwater quality data from irrigation water wells

Twenty three of 118 sampled within the study region had both cation and anion data for groundwater. The other 95 wells had only cation data available (Kresse and Fazio, 2002). Groundwater samples were labeled numerically after the initials "JEF" for Jefferson county of Arkansas. Groundwater samples for metals were filtered through a 0.45 μm pore-sized membrane and preserved with concentrated HNO_3 to a pH of 2 or less standard units. These groundwater samples were analyzed by a plasma optical-emission mass spectrometer following EPA method 200.8. Temperature, conductance, and pH were measured in the field at the time of sampling with an Orion™ multifunction portable meter. Dissolved anions including Cl^-, Br^-, F^-, SO_4^{2-}, NH_4–N, NO_3^-–N, PO_4^{3-}–P were measured on the non-acidified samples by Ion Chromatograph following standard EPA method Anion 300.0. Total organic carbon (TOC) was measured by a TOC analyzer using the liquid sample module. Table 5 shows the common chemical parameters of groundwater generated from 23 irrigation water wells in the research area. The groundwater quality data from irrigation water wells were lacking several important redox-sensitive parameters, including As and Fe speciation, DO, dissolved hydrogen sulfide, and oxidation–reduction potential. Groundwater quality data including As and Fe speciation, DO, dissolved hydrogen sulfide, and oxidation–reduction potential generated from the three pairs of nested monitoring wells in the research area were used to supplement the necessary redox-sensitive parameters. This provided the basic data necessary for more detailed interpretation about arsenic release, mobilization and transport within the alluvial aquifer.

3.10. Geochemical modeling

The surface complexation modeling (SCM) of PHREEQC (Parkhurst and Appelo, 1999) was used to predict the differences between the sorbed As in HFO derived from sequentially extracted chemical data and model simulations. The Diffuse Layer model (DLM) of Dzombak and Morel (1990) was used to simulate surface complexation reactions. The only model sorbent was selected as HFO (e.g. ferrihydrite). Hydrous aluminum and manganese oxides may be important where these oxide phases are abundant relative to HFO and under chemical conditions where HFO phases are unstable (Rochette et al., 1998). Quantitatively HFO is the dominant sorbent phase in aquifer sediments compared to hydrous Al and Mn oxide phases (Welch et al., 1999). Detailed methodology and results of SCM are presented elsewhere (Sharif, 2007).

The PHREEQC was also used for inverse geochemical modeling. Groundwater analyses data from Kresse and Fazio (2002) was used in the model, rather than groundwater data from the nested monitoring wells, as the larger data set facilitated the selection of optimal initial and final endpoints along the dominant flow path direction (NW–SE) on the high-precision water level contour map in the area. Potential phases were included into the model from XRD and SEM analysis of sediment samples. Detailed methodology and results of inverse modeling are presented in a separate paper (Sharif et al., 2008).

4. Results

4.1. Lithology

Interpretation of more than 300 water-well logs in the database of the AGC shows that the study area is overlain by an aquitard of varying thickness (<6 to 12 m) and porosity (<15 to 30%). The borehole data from the six borings completed for the present study were compared to the nearby AGC borehole data and showed good similarity between the two lithologic data sets. Spatial distribution of porosity and permeability of the surface aquitard varies significantly due to the spatial distribution of varying proportions of sand, silt, and clay size particles in the lithologic units. Interpretation of grain size analyses data from the collected cores of six borings reveals varying proportion of silty clay, silty sand, clayey silt, clayey sand, sandy silt, sand, and silt in the lithologic units. The surface aquitard at DRL1 and DRL2 sites is mainly composed of silty sand and sandy silt, as opposed to the more abundant silty clay or silt units encountered at the DRL6 site. As such, the vertical hydraulic conductivity is higher at DRL1 and DRL2 sites compared to DRL6 site. Surface aquitard thickness is 8 to 12 m in a NW–SE trending strip (a width of 5 km) with a NE–SW elongated extension in the study area (Fig. 2). Surface aquitard thickness outside this strip is <8 m. At DRL1 and DRL2 sites, the surface aquitard is <9 m below the ground surface, whereas it extends >12 m below the ground surface at DRL6 site. A sequence of medium to coarse sands with abundant gravels was encountered below the aquitard to total depth of drilling (36.5 m) at all sites. Occasional thin layers (0.1 to 0.5 m) of intercalated fine sands and silty clays were observed throughout the drilling profile. For this study, the saturated sediments below the surface aquitard are referred to as "alluvial aquifer".

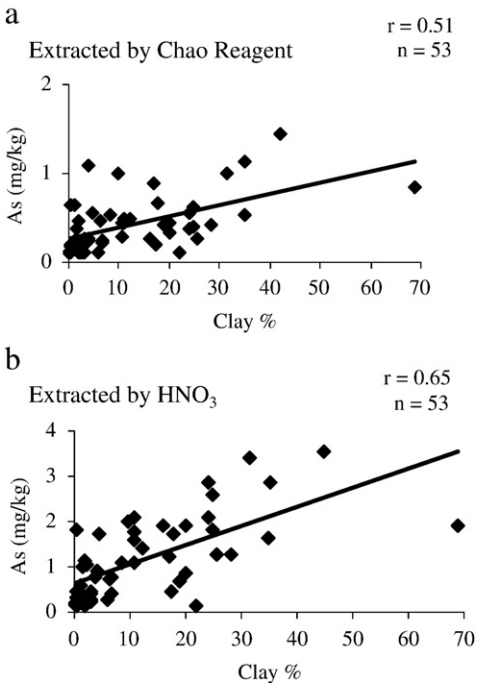

Fig. 3. Percentage of clay (clay-sized particle) is positively correlated to As in sediments. (a) A scatter plot between percentage of clay (clay-sized particle) and As (mg/kg) in sediments extracted by Chao reagent (r=0.51). (b) A scatter plot between percentage of clay (clay-sized particle) and As extracted by HNO_3 (r=0.65). Total number of sediment sample (n) is 53.

XRD analyses confirm the presence of various minerals, including quartz, orthoclase feldspar, calcite, dolomite, fluorite, gypsum, goethite, hematite, magnetite, kaolinite, ferruginous smectite, illite, and chlorite. No Al and Mn oxide phases are identified by XRD analysis. SEM analysis of magnetic minerals mostly shows a varying nature of crystallinity from fully crystalline with sharp or broken crystal faces to poorly crystalline or amorphous. SEM analysis of magnetic minerals shows the presence of both amorphous and crystalline phases of Fe oxide and oxyhydroxide minerals as separate grains as well as Fe oxide/oxyhydroxide coatings on detrital grains.

4.2. Sediment geochemistry

Arsenic extracted from amorphous Fe and Mn oxides and oxyhydroxides leached by Chao reagent varies from <0.1 to 6 mg/kg. Hot HNO_3 leachable As varies from 0.13 to 23 mg/kg with an average of 2 mg/kg. Sediments rich in clay size particles have more As compared to sediments rich in sand-sized particles in both the Chao reagent and hot HNO_3-leachable extracts. Percentage of clay (clay size particles) is positively correlated to As extracted by Chao reagent and hot HNO_3 (Fig. 3); whereas, percentage of sand is negatively correlated to As extracted from both Chao reagent and hot HNO_3 (Fig. 4). Surface aquitard and intercalated lenses in sandy aquifers rich in fine sediments are always rich in As with an average of 0.9 mg/kg extracted by Chao reagent and 2.4 mg/kg extracted by hot HNO_3, respectively. Medium- to coarse-grained sandy aquifers are low in As with an average of 0.3 mg/kg extracted by Chao reagent and 0.75 mg/kg extracted by hot HNO_3, respectively. About 20% of the total As (sum of As extracted from five steps sequential extraction) is complexed with amorphous Fe and Mn oxides and oxyhydroxides. Exchangeable As is not significant in deeper sediments (>1 m deep), but significant exchangeable As (0.04–0.07 mg/kg) is present at shallow depth (0–1 m deep) at all the three coring sites. No significant As is extracted from either carbonate or organic materials, except at shallow depth (0–1 m) in DRL1 site. The majority of the analysis of As in the sediment extracts for the exchangeable, carbonates, and organic fractions were <0.5 μg/L, which may in part be due to excess dilution of these extracts prior to analysis. The sediment extracts were diluted at a ratio of 1:30 due to exceptionally high Na^+ in the extracts, which caused build up of salts (especially Na^+) in the flow line of the ICP-MS. After accounting for the dilution factor and converting liquid concentration (μg/L) to solid-phase concentration (mg/kg), the lowest detection limit of As in the sediment were as follows: exchangeable (0.037 mg/kg), carbonates (0.375 mg/kg), amorphous Fe and Mn oxides (0.125 mg/kg), organic (0.125 mg/kg), and hot HNO_3 leachable (0.125 mg/kg). There was variation in As concentration between extraction procedures using dry and fresh wet sediments. There was no trend in the variation of As concentration between the two procedures. The variation of As concentration was ±22% in Chao reagent extracts and ±19% in hot HNO_3 extracts, respectively.

Significant Fe was extracted from both organic matter (5 mg/kg to 1.6 g/kg) and carbonates (below detection to 230 mg/kg).

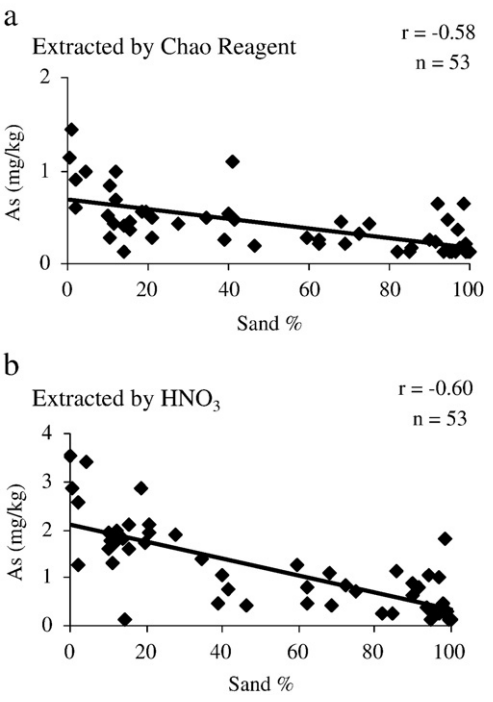

Fig. 4. Percentage of sand (sand-sized particle) is negatively correlated to As in sediments. (a) A scatter plot between percentage of sand (sand-sized particle) and As (mg/kg) in sediments extracted by Chao reagent (r=−0.58). (b) A scatter plot between percentage of sand (sand-sized particle) and As extracted by HNO_3 (−0.60). Total number of sediment sample (n) is 53.

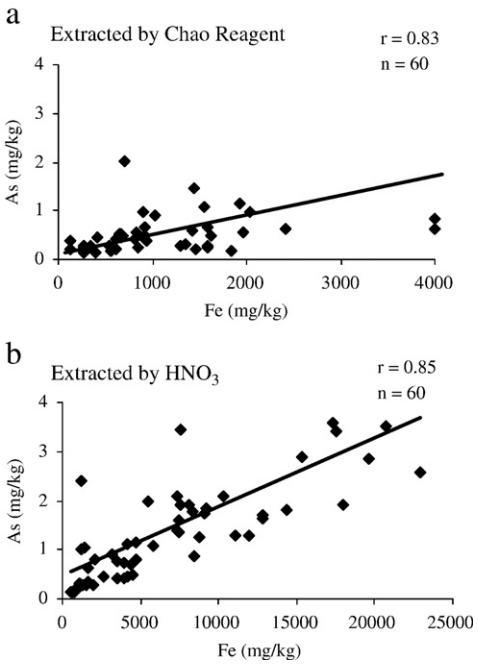

Fig. 5. Relationship between As and Fe in sediments. (a) A scatter plot between As (mg/kg) and Fe (mg/kg) in sediments extracted by Chao reagent (r=0.83). (b) A scatter plot between As (mg/kg) and Fe (mg/kg) in sediments extracted by HNO_3 (r=0.85). Total number of sediment sample (n) is 60.

Fe was also extractable from the exchangeable fraction in the range of <1 mg/kg to 26.5 mg/kg. The amount of solid-phase Fe extracted by Chao reagent and hot HNO_3 varies from 64 to 10,000 mg/kg and 500 to 23,000 mg/kg, respectively, with proportionally less Fe at depth.

4.3. Association of solid-phase As with Fe in the sediments

Arsenic is positively correlated to Fe extracted by both Chao reagent and hot HNO_3 in the sediments (Fig. 5). The ratio between the concentration of Fe extracted by Chao reagent (reducible Fe by Chao reagent or 0.25 M NH_2–OH–HCl in 0.25 M HCl) and hot HNO_3 (Fe liberated by hot HNO_3) (herein referred to as the ratio of Fe (II)/Fe) is positively correlated to depth (Fig. 6). The ratio of Fe (II)/Fe is positively correlated to As extracted by Chao reagent and negatively correlated to As extracted by hot HNO_3 (Fig. 7).

4.4. Groundwater geochemistry

Groundwater pH is predominantly near neutral to slightly alkaline (pH 6.1–7.1) with very low DO (DO 0.08–0.4 mg/L). Measurement of ORP expressed as relative millivolt (RmV) shows the research sites fall in the zone of suboxic to anoxic conditions (Langmuir et. al., 2005). Significantly mildly oxidizing to moderate reducing conditions (ORP 55–198 RmV) were observed at DRL1 (DRL1S and DRL1D) and DRL2 (DRL2S and DRL2D) sites with a relatively thin surface aquitard composed of silty sand and sandy silt. Compared to the redox zonation map of Langmuir et al. (2005), important redox reactions in this environment are considered to be: (1) reduction of NO_3^- to N_2 (2) reduction of solid Mn (IV) oxide → aqueous Mn^{2+} (3) reduction of solid Fe (III) oxide → aqueous Fe^{2+}, and (4) oxidation of organic matter.

Strongly reducing (ORP −223 to −247 RmV) conditions were detected at DRL6 (DRL6S and DRL6D) site with relatively thick surface aquitard composed of silty clay or silt. Important redox reactions in this environment are considered to be: (1) reduction of solid Fe (III) oxide → aqueous Fe^{2+} (2) reduction of SO_4^{2-} to S^{2-} (3) ammonification of N_2 → NH_4^+ (4) oxidation of organic matter, and (5) possible methanogenesis or CH_4 fermentation.

The groundwater in the area is generally Ca^{2+}–HCO_3^- type (Fig. 8) with Ca^{2+} (11–143 mg/L) and HCO_3^- (63–533 mg/L) as major cation and anion, respectively. The total dissolved solid (TDS) concentrations increase 3- to 4-fold along the dominant flow path in a south easterly direction. This large range of TDS reflects the variation of mainly HCO_3^- and Ca^{2+}, and to a lesser extent SO_4^{2-}, Cl^-, and Fe. TDS, as well as major ions (except Cl^-, SO_4^{2-}, and Fe^{2+}), are higher in each of the three shallow wells as compared to the deep counterparts for each of the nested wells. Considerable variability is noted in the concentration of Na^+ (11–72 mg/L), Mg^{2+} (4–34 mg/L), and Mn^{2+} (0.4–2.7 mg/L) in the groundwater. The concentrations of SO_4^{2-} (1–85 mg/L) and Cl^- (7–116 mg/L) are highly variable spatially. The concentration of SO_4^{2-} varies from 46 mg/L to 1.4 mg/L at DRL6 site in the shallow (DRL6S) and deep well (DRL6D), respectively. The concentration of NO_3^-–N (<0.01–2.25 mg/L) is generally low. The concentration of NH_4–N is generally low (0.03–1.1 mg/L) with the relatively high values in areas of thick surface aquitard (e.g. 1.1 mg/L at

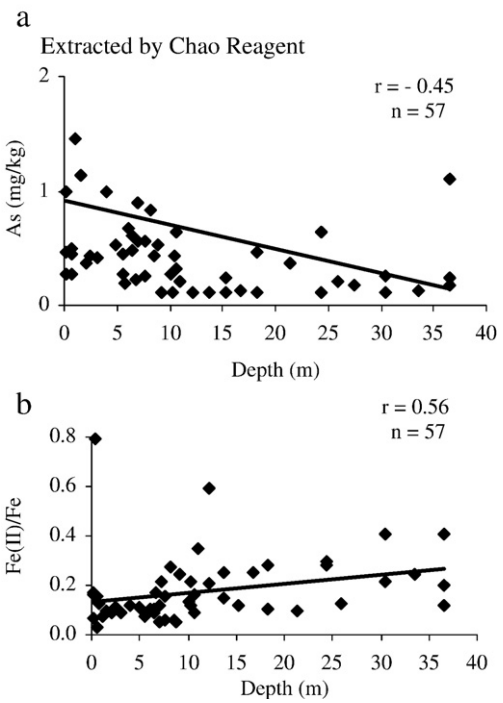

Fig. 6. Vertical distribution of As and Fe (II)/Fe in sediments. (a) A scatter plot between depth (m) and As (mg/kg) in sediments extracted by Chao reagent (r=−0.45). (b) A scatter plot between depth (m) and Fe (II)/Fe (the ratio of Fe concentration in the extracts of Chao reagent and HNO_3) in sediments (r=0.56). Total number of sediment sample (n) is 57.

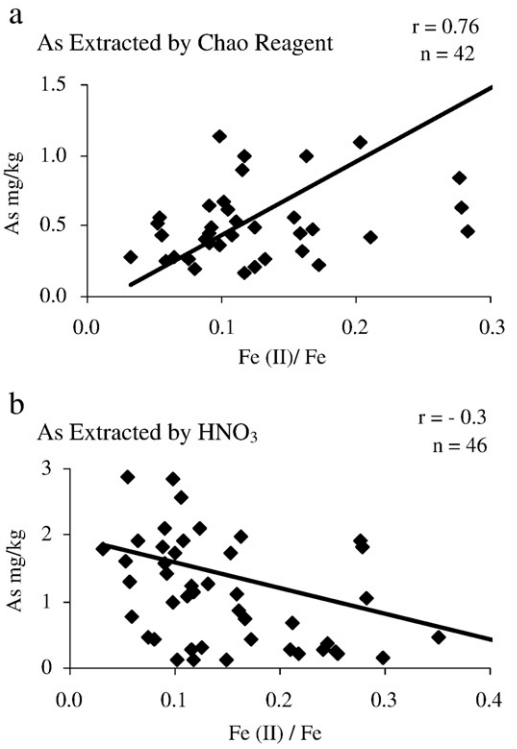

Fig. 7. Relationship between the ratio of Fe (II)/Fe and As in sediments. (a) A scatter plot between As (mg/kg) extracted by Chao reagent and Fe(II)/Fe (the ratio of Fe concentration in the extracts of Chao reagent and HNO_3) in sediments (r=0.76; n=42). (b) A scatter plot between As (mg/kg) extracted by HNO_3 and Fe(II)/Fe in sediments (r=0.3; n=46).

DRL6S). Dissolved S^{2-} is detectable in all the monitoring wells with relatively higher concentrations at the DRL2 and DRL6 sites. TOC concentrations (0.5–11 mg/L) in groundwater are highly variable. Volatile organic carbon (VOC) concentrations at the well head of DRL6S (VOC 1.4 ppm) was the highest compared to other wells (VOC<0.1–0.7 ppm) in the area.

Concentrations of Fe^{2+} in the groundwater range from 0.04 to 29 mg/L. Fe speciation data in the groundwater at three monitoring well sites show that significant Fe^{3+} (2 to 32 mg/L) is present in all the monitoring wells, with the highest concentration at DRL1D (32 mg/L). Significant particulate Fe is present in all the monitoring wells. Arsenic concentration in the area is highly variable (<0.5–77 μg/L). Speciation data of As in the groundwater at three monitoring well sites shows that As^{5+} dominates over As^{3+} in groundwater. Organic As (MMAA and DMAA) was <0.5 μg/L in all the monitoring wells. Particulate As is not significant in the groundwater. The highest As concentration (77 μg/L) was found in an irrigation water well near to DRL1 site. In the three monitoring well sites, the highest and lowest As concentration were detected in DRL6S (49.4 μg/L) and DRL1S (0.73 μg/L), respectively. A very low As concentration was recorded at DRL6D (1 μg/L). Higher concentrations of As were detected in the deep monitoring wells compared to shallow monitoring wells in DRL1 and DRL2 sites, whereas lower concentrations of As were encountered at the deep well compared to the shallow well at DRL6 site.

4.5. Association of different chemical parameters in groundwater

The concentration of ($Ca^{2+}+Mg^{2+}$ meq/L) and ($HCO_3^-+SO_4^{2-}$ meq/L) in groundwater shows that both carbonate and silicate dissolution are present in the area. Localized gypsum dissolution contributes both Ca^{2+} and SO_4^{2-} in groundwater. The Ca^{2+} released by the dissolution of gypsum leads to the precipitation of additional calcite and an increase in CO_2, which leads to a slightly lower pH and supersaturation or near equilibrium of calcite in the groundwater. This phenomenon is referred to as common ion driven precipitation or common ion effect (Back and Hanshaw, 1970; Langmuir, 1997) and is present in the area (Sharif et al., 2008). The common ion effect of gypsum dissolution and calcite precipitation is often accompanied by dolomite dissolution, leading to the observed increase in Mg^{2+} in groundwater (JEF1, JEF2, JEF3, JEF9, JEF11, JEF12, JEF13, and DRL6S). Gypsum is controlling Ca^{2+} solubility where SO_4^{2-} concentration is relatively high. An increase in Na^+/Cl^- ratios results in decreasing $(Ca^{2+}+Mg^{2+})/HCO_3^-$ ratios that are consistent with cation exchange along with high Na^+/Cl^- ratios in the groundwater. The concentrations (meq/L) of Na^+ and Cl^- in groundwater provide evidence that halite dissolution is not a major process controlling Na^+ and Cl^- in groundwater. Na^+ is comparatively higher than Cl^- in the majority of the wells, this provides evidence of silicate dissolution and cation exchange, rather than dissolution of halite (Kresse and Fazio, 2002; Sharif et al., 2008). Anaerobic decay of organic matter and SO_4^{2-} reduction (both reaction release CO_2) are controlling the SO_4^{2-} concentration in groundwater and subsequent increase in HCO_3^- and decrease in pH. HCO_3^- is always higher than equivalent Ca^{2+}, which is an indication that some HCO_3^- is also coming from processes other than calcite dissolution, or the Ca^{2+} is lost in the cation exchange reactions. Dissolution of silicate (albite) and oxidation of organic matter may have produced the excess HCO_3^- in the groundwater. The concentration of HCO_3^- has positive correlations with Ca (Fig. 9a), NH_4–N (Fig. 9b), TOC (Fig. 9c), and As (Fig. 9d).

As^{3+} positively correlates to Fe^{2+}, Fe^{3+}, and Fe^{total} in groundwater (Fig. 10a). As^{5+} shows less positive correlation to Fe^{2+}, Fe^{3+}, and Fe^{total} (Fig. 10b). Total As also shows less positive correlation to Fe^{2+}, Fe^{3+}, and Fe^{total} (Fig. 10c). Decreasing redox (RmV) positively correlated to As^{5+} and As ^{total}, whereas redox (RmV) does not correlate to As^{3+} in groundwater (Fig. 10d).

4.6. Geochemical modeling

Saturation Indices data (MINTEQA2) denotes that the groundwater system of the area is super-saturated with magnetite, pyrite, and quartz (Table 6). The area is under-saturated with respect to hematite, goethite, ferrihydrite, siderite, fluorite, halite, calcite, gypsum, barite, sphalerite, FeS (ppt). Calculation of log [{gypsum}/{(Ca^{2+})}] and log (calcite)/(Ca^{2+})] shows that gypsum is controlling Ca^{2+} solubility where dissolved SO_4^{2-} is relatively high (e.g. DRL1S and DRL6S), whereas calcite is controlling Ca^{2+} solubility in other monitoring wells where dissolved SO_4^{2-} is relatively low (e.g. DRL2S and DRL2D). Inverse geochemical modeling of PHREEQC was simulated along the dominant flow path to account for reasonable phase mole transfers that produce the changes in water chemistry along the flow path. The dissolution of HFO and precipitation of sulfide

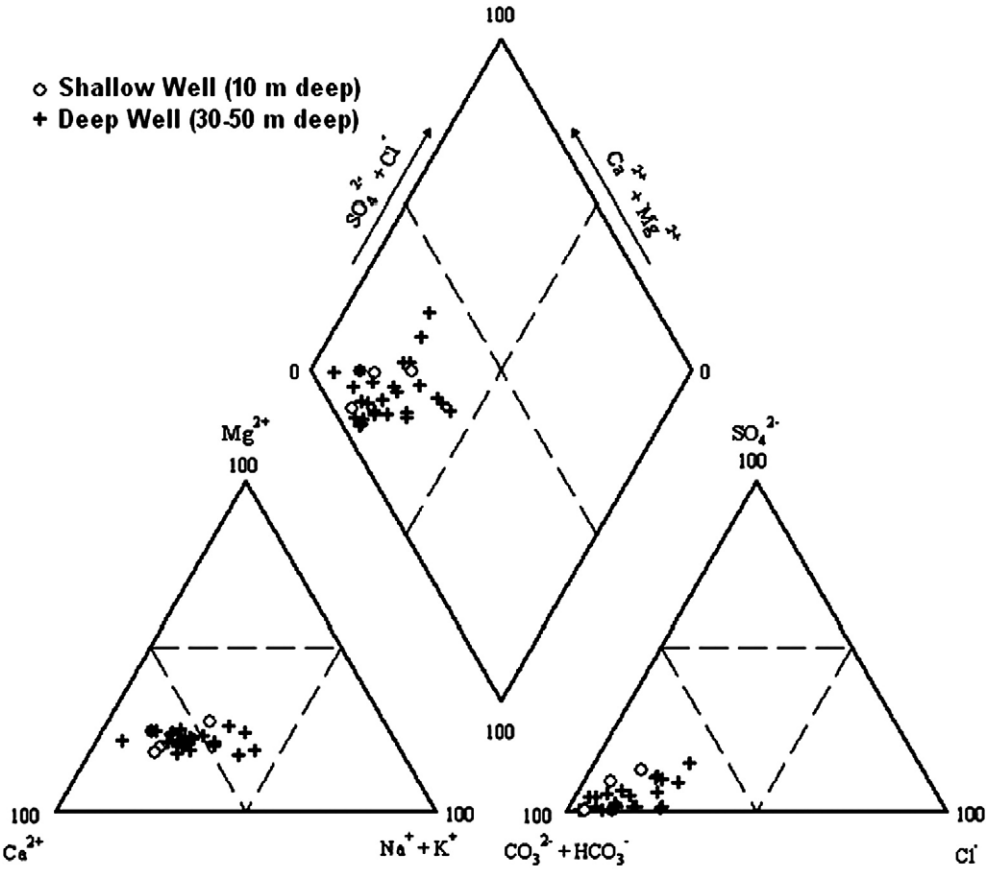

Fig. 8. Piper's (1944) diagram of the geochemical evolution of groundwater in the area.

minerals can be explained by the phase mole transfers along the flow path. The nature of dissolution and precipitation of gypsum, calcite, fluorite, barite, siderite, and cation exchange reactions are also explained by the inverse modeling along the flow path (Sharif et al., 2008).

The SCM results are quite unsatisfactory at depths of 21–36.5 m, as the model over predicts 4 to 24 times the observed sediment As, when using ferrihydrite or goethite as a potential sorbent. At depths of 0–10 m, the model predicts 53% of the observed As in sediments extracted from Chao reagent, when using ferrihydrite as the sorbent phase. At depths of 10–17 m, the model provides the best overall prediction of 92% of the observed As in sediments extracted from Chao reagent, when using ferrihydrite as the sorbent phase. At depths of 0–17 m, the model's prediction capacity is about 81% of the observed As in sediments extracted from HNO_3, when assuming goethite as the sorbent phase (Sharif, 2007).

5. Discussion

5.1. Geochemical evolution of groundwater

Geochemical evolution of groundwater in the study area is similar to that of groundwater in alluvial settings in different parts of the world (Chapelle and Lovley, 1992; Bhattacharya, 2002; O'Day et al., 2004; Jungho et al., 2006). Near the recharge area, groundwater is oxygenated. DO concentrations decrease along the flow path, presumably due to consumption by aerobic microbes (and the oxidation of organic matter). Specific types of microbial activity, most notably aerobic respiration and Fe oxide reduction, lead to a net generation of acid, but reaction of groundwater with minerals, especially carbonate minerals, in the aquifer consumes the acid, driving up pH, which controls the chemical evolution of the groundwater. The rate of microbial respiration and creation of different redox zones favorable for specific microbes is not directly dependent on the relative richness of dissolved organic matter. Instead initial fermentation has been identified as a factor limiting the rate of microbial respiration in different redox environments (Boudrea and Ruddick, 1991; Postma and Jakobsen, 1996). Once DO is depleted, groundwater enters a zone rich in dissolved Fe^{2+}, likely supplied by Fe reducing bacteria (by reducing HFO). Next, the groundwater enters a relatively Fe-poor zone in which SO_4^{2-} reducing bacteria are believed to predominate (Jungho et al., 2006). According to the inverse modeling calculation, the major processes affecting groundwater composition along the flow path are the dissolution of calcite, gypsum, barite, fluorite, HFO, cation exchange reactions of Ca^{2+} for Na^+ on exchange sites, and precipitation of sulfide (Sharif et al., 2008).

5.2. Mechanisms controlling as mobility

Total solid-phase As concentrations (an average of 2 mg/kg) measured in the study area are comparable to those measured in other As-affected areas in Bangladesh (Ahmed et al., 1998, 2004; Nickson et al., 2000; BGS & DPHE, 2001), India (Bhattacharya et al., 1997; Acharyya et al., 2000), Vietnam (Berg et al., 2001), and USA (Smedley and Kinniburgh, 2002). These ranges of solid-phase As concentrations are actually

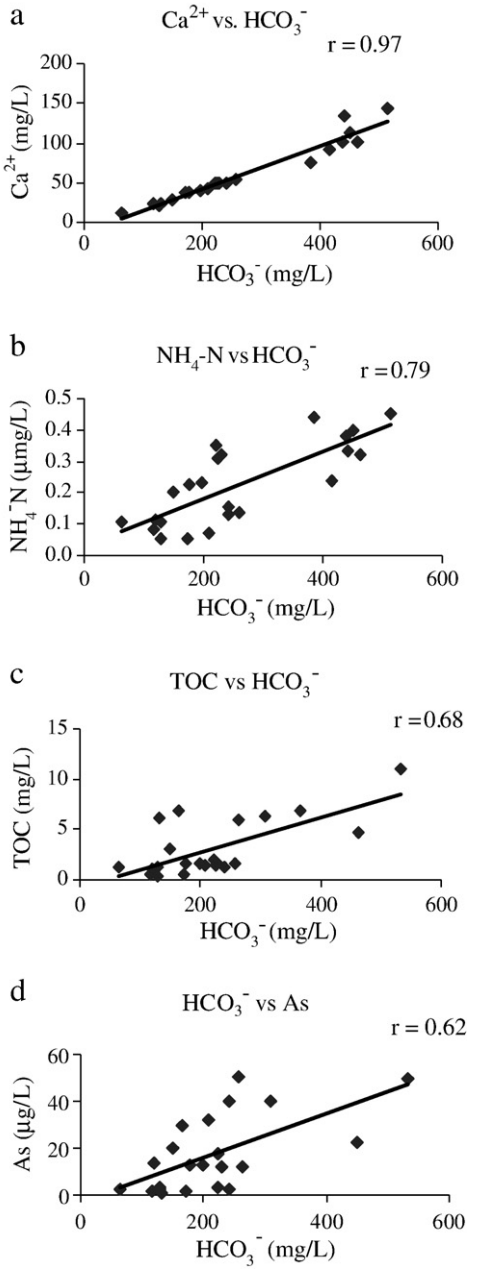

Fig. 9. Relationship between HCO_3^- and Ca^{2+}, NH_4–N, TOC, and As in groundwater. (a) A scatter plot between Ca^{2+} (mg/L) and HCO_3^- (mg/L). (b) A scatter plot between NH_4–N (mg/L) and HCO_3^- (mg/L). (c) A scatter plot between TOC (mg/L) and HCO_3^- (mg/L). (d) A scatter plot between As (µg/L) and HCO_3^- (mg/L).

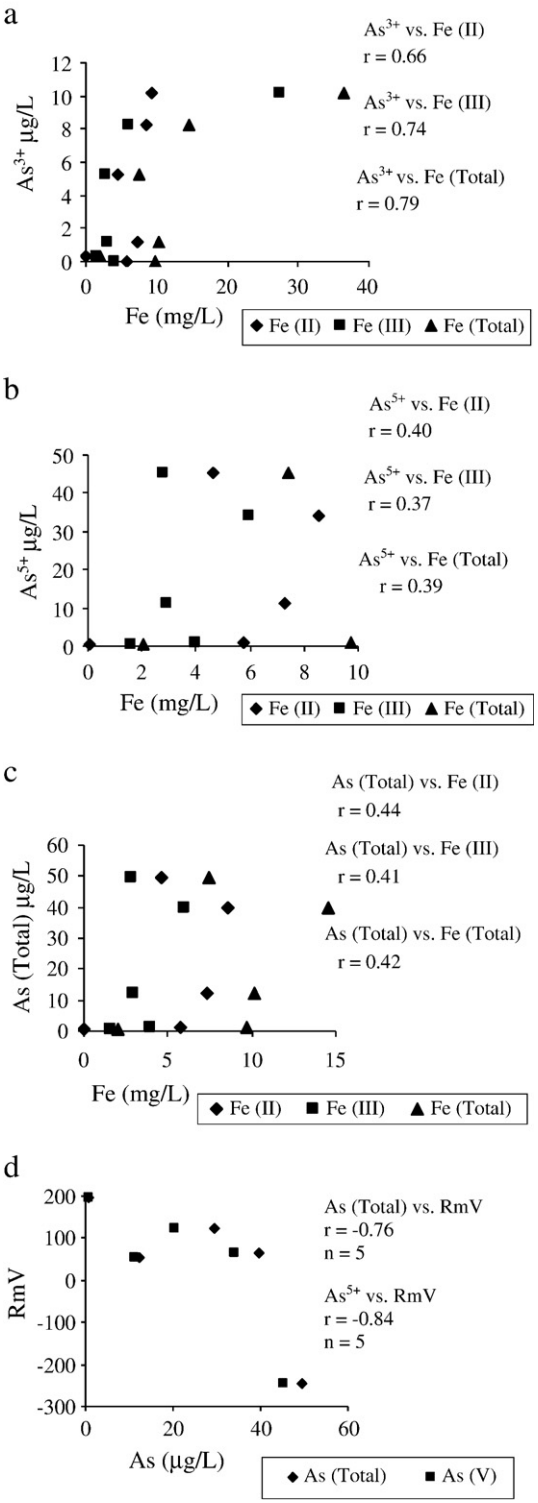

Fig. 10. Arsenic speciation and its relations to Fe speciation and redox condition in groundwater. (a) A scatter plot between As^{3+} and Fe (II), Fe (III), and Fe (Total). (b) A scatter plot between As^{5+} and Fe (II), Fe (III), and Fe (Total). (c) A scatter plot between As (Total) and Fe (II), Fe (III), and Fe (Total). (d) A scatter plot between RmV and As^{5+} and As (Total).

Table 6
Saturation Indices data of minerals (super-saturated phases are allowed to precipitate) by MINTEQA2

Minerals	DRL1S	DRL1D	DRL2S	DRL2D	DRL6S	DRL6D	JEF10	JEF13	JEF19	JEF21	JEF23
	SI	SI	SI	SI	SI	SI	SI	SI	SI	SI	SI
Sphalerite	−5.0	−4.0	−4.0	−4.0	*SS	*SS	−4.46	*SS	−5.49	*SS	−5.40
FeS (ppt)	−13	−12	−9.5	−10	−4.5	−5.0	−9.85	−2.29	−11.1	−2.65	−7.86
Ferrihydrite	−3.9	−3.9	−6.1	−6.1	−6.0	−5.9	−6.01	−6.01	−5.22	−5.78	−6.14
Goethite	−1.2	−1.2	−3.4	−3.4	−3.2	−3.1	−3.26	−3.25	−2.45	−3.02	−3.80
Hematite	*SS	*SS	−4.4	−4.3	−4.0	−3.9	−4.15	−4.14	−2.54	3.67	−4.39
Siderite	−3.9	−4.0	*SS	−0.03	*SS	−0.2	−0.29	*SS	*SS	−0.60	*SS
Fluorite	−1.8	−2.1	−1.8	−1.5	−4.5	−1.6	−1.91	−1.60	−2.80	−2.25	−2.05
Halite	−8.2	−8.2	−8.5	−8.5	−7.6	−7.9	−8.26	−8.08	−8.06	−8.40	−8.26
Calcite	−1.9	−2.2	−0.5	−0.7	*SS	−0.5	−0.58	−0.05	−0.40	−1.33	−0.92
Gypsum	−3.7	−5.4	−4.0	−3.8	−2.9	−4.7	−3.25	−2.23	−3.30	−2.96	−2.92
Manganite	−9.0	−9.5	−9.0	−9.0	−14	−14	−8.92	–	−9.83	–	−8.14
Barite	−1.0	−2.6	−1.6	−1.4	−0.4	−5.5	−0.80	*SS	−0.38	−0.28	−0.49

Pyrite, magnetite, and quartz are super-saturated in all wells.
*SS: Super-saturated.
Saturation Index (SI) = log [Ion Activity Product (IAP)] / [Equilibrium Constant (KT) at temperature T. Phases are constrained to be present either super-saturated or under-saturated. Saturation Indices were calculated by the computer program MINTEQA2 v. 1.50 (Allison et al., 1991). MINTEQA2 program uses built-in thermodynamic databases with the program itself (THERMO.DBS, TYPE6.DBS, REDOX.DBS, and GASES.DBS).

within the average crustal abundance of As reported in different parts of the world (Cullen and Reimer, 1989; Smedley and Kinniburg, 2002). This fact has led many researchers to conclude that high dissolved As concentrations in the aquifer are not due to the elevated solid-phase As concentrations in the sediments of As-affected aquifers (Nickson et al., 2000; McArthur et al., 2001, 2004).

The geochemistry of the research area is characterized by the following factors that affect aqueous As concentrations: (1) suboxic to anoxic redox conditions with no significant DO and NO_3^-–N, (2) presence of significant dissolved TOC, VOC, S^{2-}, (3) mutual exclusivity between As and SO_4^{2-} (Kresse and Fazio, 2003), general association between dissolved As species, Fe^{2+}, and NH_4–N, (5) presence of 20% total solid-phase As in amorphous Fe and Mn oxides in sediments, (6) positive correlations between solid-phase As with Fe and Fe (II)/Fe in the sediment extracts, (7) presence of amorphous HFO phases by XRD and SEM, (8) negative saturation indices of HFO phases and calcite. All these factors provide evidence for HFO reduction via respiration of organic matter, and concomitant release of sorbed and co-precipitated As into groundwater, as has been noted as the cause for As mobilization in the Holocene aquifer systems in Bangladesh, India, and other As-affected parts in the world (Bhattacharya et al., 1997, 2004; McArthur et al., 2004; Swartz et al., 2004; Zheng et al., 2004, Saunders et al., 2005).

The major contribution to increasing TDS along the flow path is primarily from the dissolution of carbonate minerals (as a reaction product of mainly HCO_3^- and Ca^{2+}), with minor contributions from SO_4^{2-}, Cl^-, Fe, and Na^+. There may be some relation to the release of these elements (increase of TDS) and the association of As in the groundwater. Significant amounts of TOC and VOC were detected in the groundwater of the study area. The present study and regional data (Aslan, 1994) show the richness of organic matter (below detection to 1% TOC) in the sediments of the Mississippi River Valley alluvial aquifer. No reduced sulfur phases (e.g. pyrite or sediment sulfide) in sediments were detected above the water table. But, reduced sulfur phases (below detection to 0.04%) in sediments were present below the water table. Significant reduced sulfur phases were also present in sands at depth. The ratio of concentrations in meq/L between HCO_3^- and ($Ca^{2+}+Mg^{2+}$) is greater than one in all the groundwater samples. An increase in Na^+/Cl^- ratios results in decreasing ($Ca^{2+}+Mg^{2+}$)/HCO_3^- ratios ($r=-0.73$), and the increase in Na^+ at the expense of Ca^{2+} provides evidence for cation exchange of Ca^{2+} and Mg^{2+} in place of Na^+ on the exchange sites (all ion concentrations are in meq/L). The possibility that at least some HCO_3^- is generated from oxidation or respiration of microbes cannot be ignored. The concentration of HCO_3^- has positive correlations with Ca^{2+}, NH_4–N, and TOC. These correlations may be explained by respiration of organic matter (TOC) producing NH_4–N and CO_2, with the later causing calcite dissolution. The degradation of organic matter, or respiration of organic matter by microbes, produces the essential electron donor (redox driver) to reduce HFO phases and release complexed As into groundwater. Mobilization of As may also occur by competition between As and HCO_3^- for the same sorption sites on HFO, as has been postulated an important cause for high dissolved As in groundwater in Bangladesh (Appelo et al., 2002). The surface complexation model simulation for the present research also shows that HCO_3^- is one of the most important competitive surface species for As on HFO phases (e.g. ferrihydrite, goethite).

5.3. Spatial and vertical distribution of as in the area

Spatial variability of As in groundwater is controlled by sediment geochemistry, recharge potential, thickness of surface aquitard, local flow dynamics, and the degree of reducing conditions in the aquifer. Lithologic heterogeneity is thought to be the most important control on the spatial variability in the distribution of As. The lithologic heterogeneity can be influenced by (1) the surface aquitard heterogeneity and variation in thickness leads to variation in recharge, localized dilution, and confinement, resulting in varying redox conditions in the aquifer affecting As release; (2) fine-grained intercalated lenses (silty clay, clayey silt, silt) in the aquifer are several orders of magnitude high in As and organic carbon compared to coarse aquifer sands and are particularly favorable to As release. There are possibilities that some well screens are located near or below

Table 7
Spatial variation of redox environments controlling dissolved As in groundwater

	DRL1S	DRL1D	DRL2S DRL2D	DRL6S	DRL6D
Redox environment controlling As release into groundwater.	No HFO reduction.	HFO reduction.	HFO reduction.	HFO and SO_4^{2-} reduction is equally important.	SO_4^{2-} reduction competes over HFO reduction.
	Mn (IV) oxide reduction. As liberated from the reduction of Mn (IV) oxide is readsorbed on the existing HFO, which ensures very low As in groundwater.	Reduction of SO_4^{2-} is present at low scale. Co-precipitation of S^{2-}, Fe^{2+} and As present at low scale, which may be an important limiting factor for As release into groundwater.	Reduction of SO_4^{2-} is present at low scale. Co-precipitation of S^{2-}, Fe^{2+} and As present at low scale, which may be an important limiting factor for As release into groundwater.	Co-precipitation of S^{2-}, Fe^{2+} and As may be an important limiting factor for As release into groundwater.	Liberated As is readsorbed on the existing HFO phases. Co-precipitation of S^{2-}, Fe^{2+} and As may be an important redox process ensures very low As into groundwater.

these lenses, whereas others are far from these lenses; (3) medium- to coarse-grained aquifer sands are generally less heterogeneous and have a spatially uniform As content. Irrigation wells can redistribute As concentrations and redox zonation by lowering water level, adding oxidants which can immobilize dissolved As, supplying organic carbon from surface or organic-rich nearby lenses, or flushing dissolved As from the nearby potential source area (where reductive dissolution of HFO is active) through the well. The presence of a mildly reducing Eh (transition between oxic and anoxic conditions), depleted DO and NO_3^-–N, presence of NH_4–N, Fe^{2+}, Mn^{2+}, As^{3+}, As^{5+} and dissolved organic carbon indicates an active zone of HFO reduction in DRL1D, DRL2S, and DRL2D sites. Complexed As is released from reductive dissolution of HFO phases into the ambient pore water or groundwater in these areas. At conditions where S^{2-} and Fe^{2+} are stable, the concentration of dissolved As may be controlled by the solubility of sulfide phases, and therefore depends on the presence and degree of SO_4^{2-} reducing conditions. Kresse and Fazio (2003) used analyses from 118 irrigation wells in the Bayou Bartholomew watershed which showed that dissolved SO_4^{2-} and As concentration were mutually exclusive on scatter plot. So, the fate of As released into groundwater by reductive dissolution of HFO is controlled by the intensity of SO_4^{2-} reducing conditions. The aquifer at DRL6 is characterized by a thick surface aquitard having low permeability and low recharge potential, resulting in more reducing conditions, as indicated by highly reducing Eh, insignificant DO and NO_3^-–N, presence of significant NH_4–N, Fe^{2+}, and S^{2-}. This condition is favorable for SO_4^{2-} reduction and concomitant co-precipitation of dissolved As into sulfide phases (DRL6S). Further stronger reducing condition supports a redox environment where SO_4^{2-} reduction out competes HFO reduction, and all dissolved As can be sequestered into solid sulfide (DRL6D). Table 7 shows a brief description of the spatial variation of redox environments controlling dissolved As in groundwater at the three monitoring well sites.

The surface complexation model was relatively successful in predicting As in sediments at shallow depth where sediments are mostly fine-grained. But, the model was quite unsatisfactory for the deep sandy sediments.

6. Conclusion

The recharge potential, variation of lithology, thickness and permeability of the surface aquitard, irrigation pumping, and local flow dynamics have positive relations to the spatial and vertical distribution of redox zones in the subsurface. The spatial and vertical distribution of redox zones is one of the most important factors controlling the spatial, vertical, and temporal variation of As in groundwater. Significant total As (20%) is complexed with amorphous HFO and Mn Oxides throughout the depth profile. Arsenic is not significant in carbonate and organic materials. Significant exchangeable As is present at shallow depth at all sites. As is positively correlated to Fe extracted by Chao reagent and hot HNO_3. Increasing depth has positive relation to the ratio of Fe (II)/Fe, but it has negative relation to As extracted by Chao reagent. The ratio of Fe (II)/Fe is positively correlated to As extracted from Chao reagent. Although the ratio of Fe (II)/Fe increases with depth, the amount of reducible Fe (extracted by Chao reagent) decreases noticeably with depth. So, the amount of reducible or active HFO, as well as complexed As decreases with depth. Possibilities of historic flushing of significant labile As and Fe derived from reductive dissolution of HFO by advective transport, and having less sorbing capacity of HFO phases due to loss of surface area and reactive surface sites caused by increasing crystallinity (ferrihydrite to goethite) over time at depth can not be ignored. Gypsum solubility led by common ion effect and simultaneous SO_4^{2-} reduction are controlling the amount of dissolved SO_4^{2-} in groundwater. As^{+5} and Fe^{2+} species dominate in the groundwater. Arsenic is released as As^{+5} into groundwater, part of which is later reduced to As^{+3} in a more strongly reducing environment (Zobrist et al., 2000; Stollenwerk, 2003). Although particulate As is very low, significant particulate Fe is present, which may facilitate co-transfer of As through groundwater flow or recharge into deep aquifers.

Different redox zones are characteristic in the area. At DRL1S, it is anticipated that HFO reduction is not an important redox reaction in the groundwater, while some Mn (IV) oxide may undergo reductive dissolution. The presence of the highest amount of Mn^{2+} and very low Fe^{2+} in the well signify dissolution of Mn (IV) oxide. Any As liberated from the reductive dissolution of Mn (IV) oxide is readsorbed on the existing HFO phases which ensures very low As concentration in well DRL1S. DRL1D and DRL6D are characterized by reduction of HFO with simultaneous reduction of SO_4^{2-}. DRL2 (DRL2S and DRL2D) is characterized by reduction of HFO with some degree of SO_4^{2-} reduction. The presence of significant amounts of dissolved S^{2-} and Fe^{2+} in DRL2 and DRL6 indicates that SO_4^{2-} reduction and co-precipitation of sulfide and As might be an important limiting process of

dissolved As into groundwater at these sites. The relative rate of HFO reduction over SO_4^{2-} reduction with simultaneous co-precipitation of As into sulfide phase is the dominant biogeochemical redox reactions controlling dissolved As in groundwater. In the presence of abundant reactive HFO minerals, Fe^{3+} reducing bacteria may out-compete SO_4^{2-} reducing bacteria (Kirk et al., 2004). The relatively high rate of HFO reduction over SO_4^{2-} reduction ensures high As concentration in the groundwater at DRL1D, DRL2S, DRL2D, and DRL6S. Again, if the amount of reactive HFO is limited, a mixed metabolic redox zone may develop that allows simultaneous HFO and SO_4^{2-} reduction, or SO_4^{2-} reduction to dominate over HFO reduction (Kirk et al., 2004). Very low As concentration in DRL6D can be explained by the later geochemical process where SO_4^{2-} reduction dominates over HFO reduction, and sulfide mineral formation results in subsequent co-precipitation of As into sulfide phases.

The geochemical data of sediment and groundwater indicates that reductive dissolution of amorphous HFO is the dominant process of As release in the study area. Relative redox state controls the rate and intensity of HFO reduction and the amount of As released into groundwater.

References

Acharyya, S.K., Lahiri, S., Raymahashay, B.C., Bhowmic, A., 2000. Arsenic toxicity of groundwater in parts of the Bengal Basin of India and Bangladesh: the role of Quaternary stratigraphy and Holocene sea level fluctuation. Environ. Geol. 39, 1127–1137.

Ahmed, K.M., Hoque, M., Hasan, M.K., Ravenscroft, P., Chowdhury, L.R., 1998. Origin and occurrence of water well methane gas in Bangladesh aquifers. J. Geol. Soc. India 51, 697–708.

Ahmed, K.M., Bhattacharya, P., Hasan, M.A., Akhter, S.H., Alam, S.M.M., Bhuiyan, M.A.H., Imam, M.B., Khan, A.A., Sracek, O., 2004. Arsenic enrichment in groundwater of the alluvial aquifers in Bangladesh: an overview. Appl. Geochem. 19, 181–200.

Allison, J.D., Brown, D.S., Novo-Gradac, K.J., 1991. MINTEQA2/PRODEFA2, A Geochemical Assessment Model for Environmental Systems: Version 3.0 User's Manual. US Environmental Protection Agency, Athens, GA. EPA/600/3-91/021.

Appelo, C.A.J., Van Der Weiden, M.J.J., Tournassat, C., Charlet, L., 2002. Surface complexation of ferrous iron and carbonate on ferrihydrite and the mobilization of arsenic. Environ. Sci. Technol. 36, 3096–3103.

Aslan, A., 1994. Holocene sedimentation, soil formation, and floodplain evolution of the Mississippi River Floodplain, Ferriday, Louisiana. Doctoral dissertation, Dept. of Geological Sciences, University of Colorado, 249–250.

Back, W., Hanshaw, B.B., 1970. Comparison of chemical hydrology of Florida and Yucatan. J. Hydrol. 10, 360–368.

Berg, M., Tran, H.C., Nguyen, T.C., Pham, H.V., Schertenleib, R., Giger, W., 2001. Arsenic contamination of groundwater and drinking water in Vietnam: a human health threat. Environ. Sci. Technol. 35, 2621–2626.

BGS, DPHE, 2001. Arsenic contamination of groundwater in Bangladesh. In: Kinniburgh, D.G., Smedley, P.L. (Eds.), British Geological Survey Report WC/00/19. British Geological Survey, Keyworth, UK.

Bhattacharya, P., 2002. Arsenic contaminated groundwater from the sedimentary aquifers of South-East Asia. In: Bocanegra, E., Martinez, D., Massone, H. (Eds.), Groundwater and Human Development, Proc. XXXII IAH and VI ALHSUD Congress, Mar del Plata, Argentina, 21–25 October 2002, pp. 357–363.

Bhattacharya, P., Chatterjee, D., Jacks, G., 1997. Occurrence of arsenic-contaminated groundwater in alluvial aquifers from delta plains, eastern India: options for safe drinking water supply. Water Res. Dev. 13, 79–92.

Bhattacharya, P., Welch, A.H., Ahmed, K.M., Jacks, G., Naidu, R., 2004. Arsenic in groundwater of sedimentary aquifers. Appl. Geochem. 19 (2), 163–167.

Boudreau, B.P., Ruddick, B.R., 1991. On a reactive continuum representation of organic matter diagenesis. Am. J. Sci. 291, 507–538.

Canfield, D.E., Raiswell, R., Westrich, J.T., Reaves, C.M., Berner, R.A., 1986. The use of chromium reduction in the analysis of reduced inorganic sulfur in sediments and shales. Chem. Geol. 54, 144–159.

Chapelle, F.H., Lovley, D.R., 1992. Competitive exclusion of sulfate reduction by Fe (III)-reducing bacteria: a mechanism for producing discrete zones of high-iron groundwater. Ground Water 30 (1), 29–36.

Chao, T.T., Zhou, L., 1983. Extraction techniques for selective dissolution of amorphous iron oxides from soils and sediments. Soil Sci. Soc. Am. J. 47, 225–232.

Cullen, W.R., Reimer, K.J., 1989. Arsenic speciation in the environment. Chem. Rev. 89, 713–764.

Dzombak, D.A., Morel, F.M.M., 1990. Surface Complexation Modeling: Hydrous Ferric Oxide. John Willey and Sons, Toronto.

Edwards, M., Patel, S., McNeill, L., Hsiao-wen, Chen, Frey, M., Eaton, A.D., Antweiler, R.C., Taylor, H.E., 1998. Considerations in As analysis and speciation: a modified field technique can quantify particulate As, soluble As (III), and soluble As (V) in drinking water. J. AWWA 90 (3), 103–113.

Freiwald, D.A., 1985. Average annual precipitation and runoff for Arkansas, 1951–1980. U.S. Geological Survey Water Resources Investigation Report 84-4363. 1 sheet.

Grabinski, A.A., 1981. Determination of arsenic (III), arsenic (V), monomethylarsonate, and dimethylarsinate by ion-exchange chromatography with flameless atomic absorption spectrometric detection. Anal. Chem. 53, 966–968.

Joseph, R.L., 1999. Status of water levels and selected water quality conditions in the Mississippi River Valley alluvial aquifer in eastern Arkansas. U.S. Geological Survey Water Resources Investigation Report 99-4035, p. 54.

Jungho, P., Sanford, R.A., Bethke, C.M., 2006. Geochemical and microbiological zonation of the Middendorf aquifer, South Carolina. Chem. Geol. 230, 88–104.

Kirk, M.F., Holm, T.R., Park, J., Jin, Q., Sanford, R.A., Fouke, B.W., Bethke, C.M., 2004. Bacterial sulfate reduction limits natural arsenic contamination of groundwater. Geology 32, 953–956.

Kleiss, B.A., Coupe, R.H., Gonthier, G.J., Justus, B.G., 2000. Water quality in the Mississippi Embayment, Mississippi, Louisiana, Arkansas, Missouri, Tennessee, and Kentucky, 1995–1998. U.S. Geol. Surv. Circ. 1208, 5–6.

Korte, N., 1991. Naturally occurring arsenic in ground waters of the Midwestern United States. Environ. Geol. Water Sci. 18, 137–141.

Kresse, T.M., Fazio, J.A., 2002. Pesticides, water quality and geochemical evolution of groundwater in the alluvial aquifer, Bayou Bartholomew Watershed, Arkansas. Water Quality Report WQ02-05-1, Little Rock, AR. Arkansas Department of Environmental Quality.

Kresse, T.M., Fazio, J.A., 2003. Occurrence of arsenic in groundwaters of Arkansas and implications for source and release mechanisms. Water Quality Report WQ03-03-01, Little Rock, AR. Arkansas Dept. of Environmental Quality.

Langmuir, D., 1997. Aqueous Environmental Geochemistry. Prentice Hall, Inc, Upper Saddle River, NJ.

Langmuir, D., Chrostowski, P., Vigneault, B., Chaney, R., 2005. Issue paper on the environmental chemistry of metals. U. S. EPA Risk Assessment Forum, p. 39. http://cfpub.epa.gov/ncea/cfm/recordisplay.cfm?deid=86119.

Matisoff, G., Khourey, C.J., Hall, J.F., Varnes, A.W., Strain, W.H., 1982. The nature and source of arsenic in northeastern Ohio ground water. Groundwater 20, 446–456.

McArthur, J.M., Ravenscroft, P., Safiullah, S., Thirlwall, M.F., 2001. Arsenic in groundwater: Testing pollution mechanisms for sedimentary aquifers in Bangladesh. Water Resour. Res. 37 (1), 109–117.

McArthur, J.M., Banerjee, D.M., Hudson-Edwards, K.A., Mishra, R., Purohito, R., Ravenscroft, P., Cronin, A., Howarth, R.J., Chatterjee, A., Talukder, T., Lowry, D., Houghton, S., Chadha, D.K., 2004. Natural organic matter in sedimentary basins and its relation to arsenic in anoxic groundwater: the example of West Bengal and its worldwide application. Appl. Geochem. 19, 1255–1293.

Miller, G.P., 2001. Surface complexation modeling of arsenic in natural water and sediment systems. Doctoral Dissertation, New Mexico Institute of Mining and Technology, New Mexico, USA.

Miller, W.P., Miller, D.M., 1987. A micro-pipette method for soil mechanical analysis. Commun. Soil Sci. Plant Anal. 18 (1), 1–15.

Nickson, R., McArthur, J.M., Ravencroft, P., Burgess, W.G., Ahmed, K.M., 2000. Mechanism of arsenic release to ground water, Bangladesh and West Bengal. Appl. Geochem. 15, 403–411.

O'Day, P.A., Vlassopoulos, D., Root, R., Rivera, N., 2004. The influence of sulfur and iron on dissolved arsenic concentrations in shallow subsurface under changing redox conditions. PNAS 101 (38), 13703–13708.

Parkhurst, D.L., Appelo, C.A.J., 1999. User's guide to PHREEQC (ver.2) — a computer program for speciation, batch-reaction, one-dimensional transport, and inverse geochemical calculations. U.S. Geol. Survey Water Resources Inv. Report 99-4259.

Piper, A.M., 1944. A graphical interpretation of water — analysis. Trans. - Am. Geophys. Union 25, 914–928.

Postma, D., Jakobsen, R., 1996. Redox zonation-equilibrium constants on the Fe (III)/ SO_4^{2-} reduction interface. Geochim. Cosmochim. Acta. 60 (17), 3169–3175.

Rochette, E.A., Li, G.C., Fendorf, S.E., 1998. Stability of arsenate minerals in soil under biotically generated reducing conditions. Soil, Sci. Soc. Am. J. 62, 1530–1537.

Saunders, J.A., Mohammad, S., Korte, N.E., Lee, M.-K., Castle, D., Barnett, M.O., Fayek, M., Riciputi, L., 2005. Groundwater geochemistry, microbiology

and mineralogy in two arsenic-bearing Holocene alluvial aquifers from the USA. In: O'Day, et al. (Ed.), Advances in Arsenic Research: Integration of Experimental and Observational Studies and Implication of Mitigation. Am. Chem. Soc. Symp. Series, vol. 915, pp. 191–205.

Schrader, T.P., 2001. Status of water levels and selected water quality conditions in the Mississippi River alluvial aquifer in eastern Arkansas, 2000. U.S. Geological Survey Water Resources Investigation Report 01-4124, p. 5.

Sharif, M.U., 2007. Hydrochemical evolution of arsenic in groundwater: sources and sinks in the Mississippi River Valley alluvial aquifer, southeastern Arkansas, USA. Doctoral Dissertation, University of Arkansas, Arkansas, USA.

Sharif, M.U., Davis, R.K., Steele, K.F., Kim, B., Kresse, T.M., Fazio, J.A., 2008. Inverse geochemical modeling of groundwater evolution with emphasis on arsenic in the Mississippi River Valley alluvial aquifer, Arkansas, USA. J. Hydrol. 350, 41–55.

Shelton, L.R., Chapel, P.D., 1994. Guidelines for collecting and processing samples of stream bed sediment for analysis of trace elements and organic contaminants for the National Water-Quality Assessment (NAWQA) Program. USGS Open File Report 94-458.

Smedley, P.L., Kinniburgh, D.G., 2002. A review of the source, behavior and distribution of arsenic in natural waters. Appl. Geochem. 17, 517–568.

Stollenwerk, K.G., 2003. Geochemical processes controlling transport of arsenic in groundwater: A review of adsorption. In: Welch, A.H., Stollenwerk, K.G. (Eds.), Arsenic in Ground Water: Geochemistry and occurrence, pp. 67–100.

Swartz, C.H., Keon, N.E., Badruzzaman, B., Ali, A., Brabender, D., Jay, J., Besancon, J., Islam, S., Hemond, H.F., Harvey, C.F., 2004. Mobility of arsenic in Bangladesh aquifer: inferences from geochemical profiles, leaching data, and mineralogical characterization. Geochim. Cosmochim. Acta. 68 (22), 4539–4557.

Tessier, A., Campbell, P.G.C., Bisson, M., 1979. Sequential extraction procedure for the speciation of particulate trace metals. Anal. Chem. 51 (7), 844–851.

U.S. EPA, 2001. 40 CFR Parts 9, 141, and 142, National Primary Drinking Water Regulations; Arsenic and clarification to compliance and new source contaminants monitoring; Final rule, in Federal register, 66(14), January 22, 2001.

Wayne, W.L., Franceska, D.W., Michael, T.K., 1997. Guidelines and standard procedures for studies of ground-water quality: selection and installation of wells, and supporting documentation. U.S. Geological Survey Water Resources Investigation Report 96-4233.

Welch, A.H., Helsel, D.R., Focazio, M.J., Watkins, S.A., 1999. Arsenic in groundwater supplies of the United States. In: Chappell, W.R., Abernathy, C.O., Caldedron, R.L. (Eds.), Arsenic Exposure and Health Effects. Elsevier, Amsterdam, pp. 9–17.

Zheng, Y., Stute, M., Van Geen, A., Gavrieli, I., Dhar, R., Simpson, H.J., Schlosser, P., Ahmed, K.M., 2004. Redox control of arsenic mobilization in Bangladesh groundwater. Appl. Geochem. 19, 201–214.

Zobrist, J., Dowdle, P.R., Davis, J.A., Oremland, R.S., 2000. Mobilization of arsenite by dissimilatory reduction of adsorbed arsenate. Environ. Sci. Technol. 34, 4747–4753.